The Teton – Wind River domain: a 2.68–2.67 Ga active margin in the western Wyoming Province[1]

B. Ronald Frost, Carol D. Frost, Mary Cornia, Kevin R. Chamberlain, and Robert Kirkwood

Abstract: The Archean rocks in western Wyoming, including the Teton Range, the northern Wind River Range, and the western Owl Creek Mountains, preserve a record of a 2.68–2.67 Ga orogenic belt that has many of the hallmarks of modern plate tectonics. A 2683 Ma tholeiitic dike swarm is undeformed and unmetamorphosed in the western Owl Creek Mountains. In the Wind River Range, these dikes have been deformed and metamorphosed during thrusting along the west- to southwest-directed Mount Helen structural belt, which was active at the time that the 2.67 Ga Bridger batholith was emplaced. In the northern Teton Range, the Moose Basin gneiss, which contains relict granulite-facies assemblages, appears to have been thrust upon the amphibolite-grade layered gneiss. The syntectonic Webb Canyon orthogneiss was intruded into the thrust at or before 2673 Ma. We interpret these relations, along with isotopic data indicating that the layered gneiss in the Teton Range consists of juvenile components, to indicate that the western Wyoming Province was the site of active margin tectonics at 2.68–2.67 Ga. This involved a magmatic arc in the present Wind River Range and back-arc spreading in the Owl Creek Mountains. The immature, juvenile layered gneiss in the Teton Range probably represents an accretionary prism or fore-arc basin onto which high-pressure rocks containing a mature sedimentary sequence were thrust at 2.67 Ga. Although it may be questioned as to when modern-style plate tectonics began in other cratons, it was certainly operating in the Wyoming Province by 2.67 Ga.

Résumé : Les roches archéennes dans l'ouest du Wyoming, incluant la chaîne Teton, le nord de la chaîne Wind River et les Monts Owl Creek occidentaux, enregistrent une ceinture orogénique, 2,68 – 2,67 Ga qui présente plusieurs caractéristiques de la tectonique des plaques moderne. Dans les monts Owl Creek occidentaux, on retrouve un essaim de dykes tholéiitiques, 2683 Ma, non déformé ni métamorphisé. Dans la chaîne Wind River, ces dykes ont été déformés et métamorphisés durant un chevauchement le long de la ceinture structurale Mount Helen, de direction W à SW; cette ceinture était active au moment de la mise en place du batholite Bridger, 2,67 Ga. Dans le nord de la chaîne Teton, le gneiss de Moose Basin, contenant des assemblages reliques au faciès des granulites, semble avoir été chevauché sur le gneiss stratifié, lequel est au grade des amphibolites. L'orthogneiss syntectonique de Webb Canyon a été introduit dans le chevauchement vers 2673 Ma ou plus tôt. Nous interprétons ces relations, ainsi que les données isotopiques indiquant que le gneiss stratifié de la chaîne Teton est formé de composantes juvéniles, comme une indication que la Province de Wyoming occidentale a été un site tectonique de bordure active vers 2,68 – 2,67 Ga. Cela implique un arc magmatique dans la présente chaîne Wind River et un arrière-arc qui s'étendait dans les Monts Owl Creek. Les gneiss stratifiés, juvéniles et immatures dans la chaîne Teton représentent probablement un prisme d'accrétion ou un bassin d'avant arc sur lequel des roches à pression élevée contenant une séquence sédimentaire mature ont été chevauchées, il y a 2,67 Ga. Bien que l'on puisse se demander à quel moment la tectonique des plaques de style moderne a débuté dans d'autres cratons, elle était certainement active dans la Province de Wyoming il y a 2,67 Ga.

[Traduit par la Rédaction]

Introduction

Although modern plate tectonics have been used for years to model the development of Archean continents (e.g., Ellis 1992; Windley 1993), there is still considerable dispute as to when modern-style plate tectonics began (Hamilton 1998). The circular outcrop pattern of batholiths in middle Archean terranes surrounded by greenstone belts is strong evidence that vertical tectonics dominated early in Earth's history (Van Kranendonk et al. 2004). Many maintain that vertical tectonics were prevalent nearly to the end of the Archean (Hamilton 1998; Bédard et al. 2003; Rey et al. 2003) but

Received 18 August 2005. Accepted 31 August 2006. Published on the NRC Research Press Web site at http://cjes.nrc.ca on 6 January 2007.

Paper handled by Associate Editor L. Corriveau.

B.R. Frost,[2] C.D. Frost, M. Cornia, K.R. Chamberlain, and R. Kirkwood. Department of Geology and Geophysics, University of Wyoming, Laramie, WY 82071, USA.

[1]This article is one of a selection of papers published in this Special Issue on *The Wyoming Province: a distinctive Archean craton in Laurentian North America.*

[2]Corresponding author (rfrost@uwyo.edu).

 doi:10.1139/E06-102

Fig. 1. Geologic map of the Wyoming Province showing the outcrop of Precambrian rocks. Line A–A′ is the approximate line for the geologic sketch in Fig. 13. MHSB, Mount Helen structural belt; OTSB, Oregon Trail structural belt.

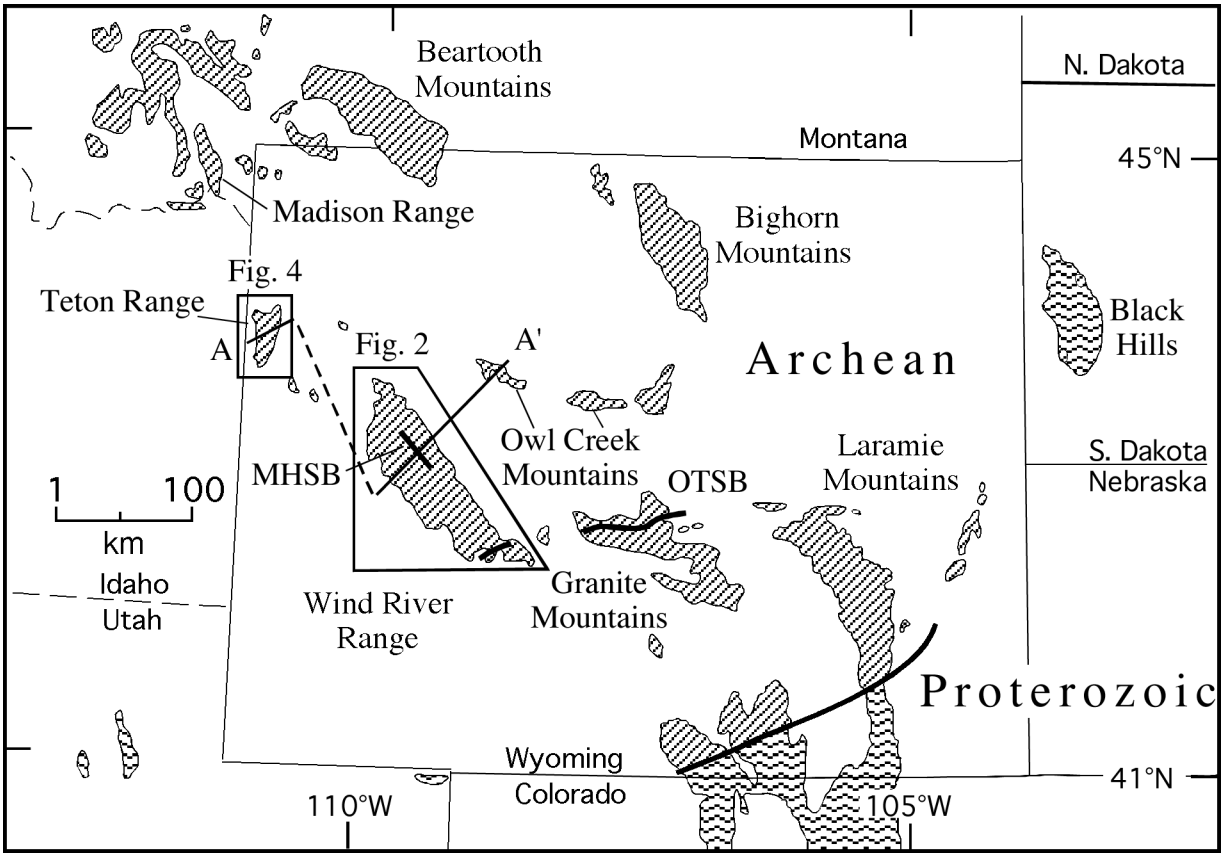

others postulate that modern-style plate tectonics was operating at least by the middle Archean (Card 1990; Barton et al. 1992; Percival and Skulski 2000). In an earlier paper, we noted that the 2.7–2.63 Ga batholiths in the Wyoming Province have a distinct linear arrangement and that they probably represent the remnants of a Neoarchean magmatic arc (Frost et al. 1998). Here we present the results of further work in the western Owl Creek Mountains (Kirkwood 2000), Wind River Range, and Teton Range (Cornia 2003) that demonstrate that the a 2.70–2.67 Ga orogeny in western Wyoming Province was associated with back-arc rifting, high-pressure metamorphism, contractional deformation, and calc-alkalic magmatism—all hallmarks of modern-day plate tectonics.

Regional geology of the Wyoming Province

The Archean Wyoming Province is exposed in a series of Laramide uplifts in Wyoming and southwestern Montana (Fig. 1). Chamberlain et al. (2003) summarized the available geochronology for the province and subdivided it into three major subprovinces. The center of the province is the Bighorn subprovince, which consists of granitic and tonalitic gneisses that have not been metamorphosed since ca. 2.8 Ga (Frost et al. 2006*a*). Abutting the Bighorn subprovince to south and west is the Sweetwater subprovince, wherein the granites and gneisses record deformation and magmatism ranging from 2.7 to 2.5 Ga. The northwestern portion of the Wyoming Province is the Montana metasedimentary province (MMP), which was tectonically juxtaposed against the rest of the province around 2.5 Ga (Mogk et al. 1992). Our recent work has shown that the Sweetwater subprovince consists of at least two structural domains, one centered on the Granite Mountains, dominated by the east–west-trending Oregon Trail structural belt (Grace et al. 2006), the second centered on the Teton and Wind River ranges. In this paper, we will describe the structure, petrology, geochronology, and geochemistry of gneisses in Wind River and Teton ranges (Fig. 1) and argue that they share a common late-Archean history that is distinct from the rest of the Wyoming Province.

Western Owl Creek Mountains

The Owl Creek Mountains, a small Laramide uplift that lies about 65 km northeast of the Wind River Range (Fig. 1), are divided into two parts by the Wind River Canyon. The Archean rocks in the eastern Owl Creek Mountains consist of a ca. 2.9 Ga supracrustal belt that has been intruded by 2.6 Ga peraluminous granite (Hausel et al. 1985; Mueller et al. 1985; Hedge et al. 1986; Stuckless et al. 1976). The Archean rocks in the western Owl Creek Mountains consist of tonalitic basement gneisses (Kirkwood 2000) that are the same age and compositionally similar to the granites and gneisses in the Bighorn Mountains and the Washakie block of the Wind River Range (Frost et al. 2006*a*). The gneisses of the western Owl Creek Mountains have been cut by a mafic dike swarm that trends in a roughly northwesterly di-

Fig. 2. Geologic map of the northern Wind River Range.

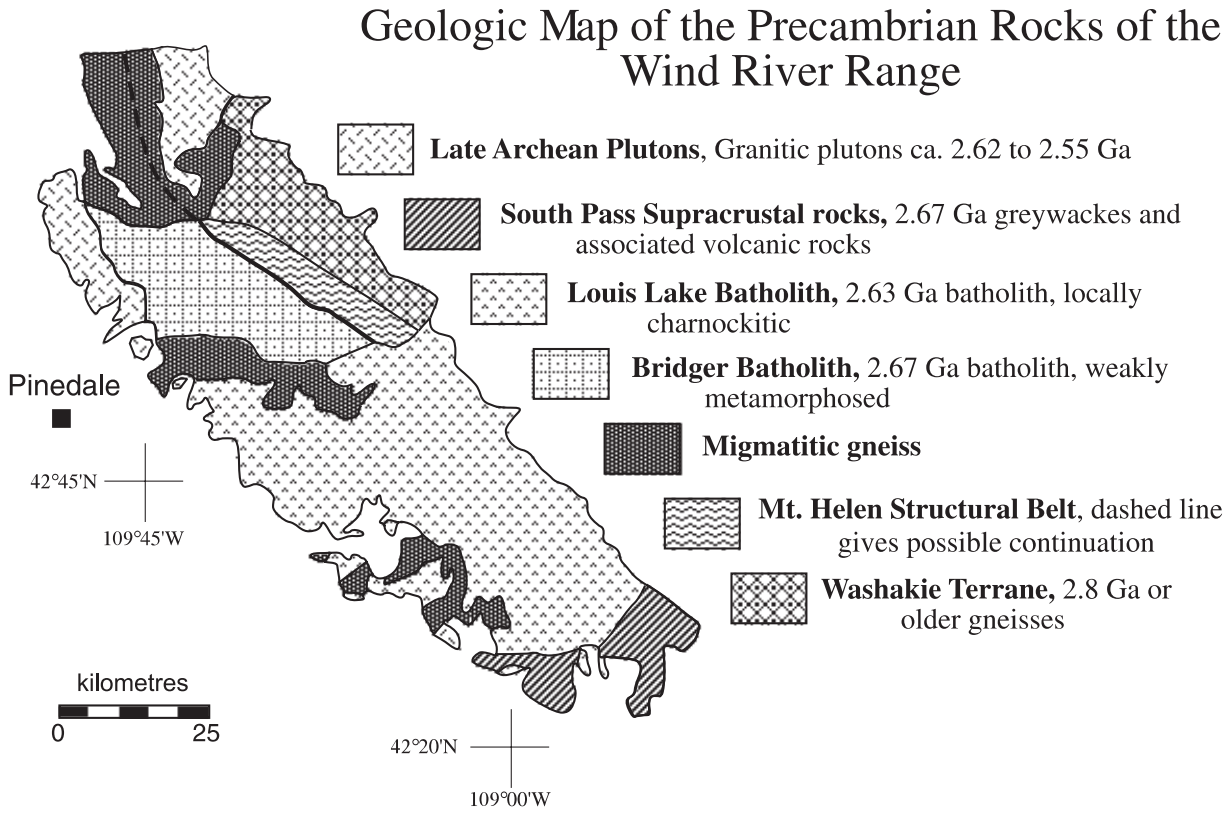

Fig. 3. Block diagram showing relationship between the Bridger batholith and the Mount Helen structural belt. Width of block is about 5 km. Key features include (1) footwall of MHSB consists of gneisses similar in appearance to the 2.84 Ga Native Lake gneiss, (2) mafic rocks form boudins within the MHSB that have granulite-facies assemblages in the core and amphibolite-facies assemblages in the rims, (3) early dikes of the Bridger granite are folded in the MHSB, (4) main phase of the Bridger batholith truncates the MHSB, but carries (5) the same foliation.

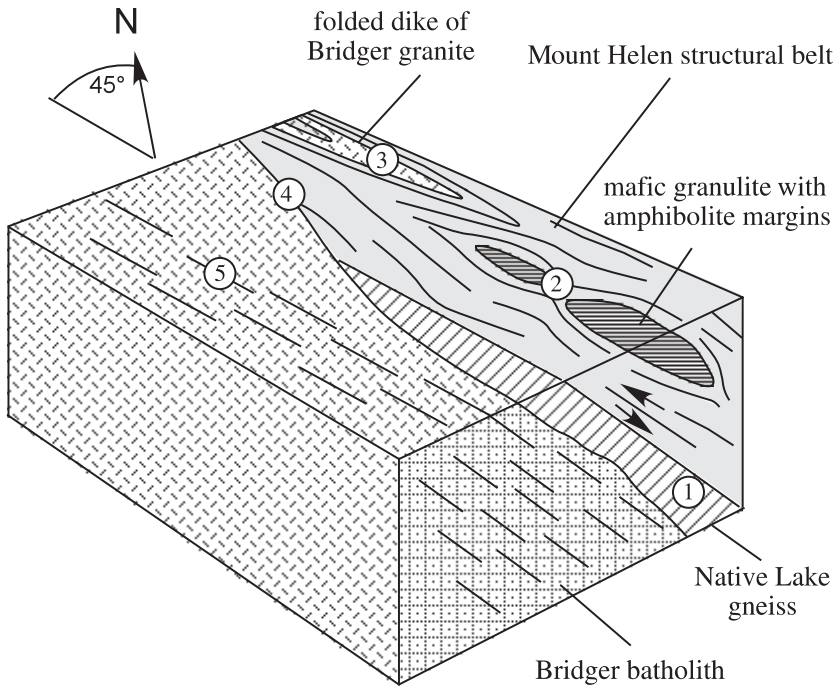

rection (Kirkwood 2000). One of these undeformed and unmetamorphosed dikes has been dated as part of this study.

Wind River Range

The gneisses in the Wind River Range show a long, complex history of plutonism, deformation, and metamorphism that spans from at least 2.9 to 2.55 Ga (Koesterer et al. 1987; Frost et al. 1998; Frost et al. 2000*a*, 2000*b*; Frost et al. 2006*b*). Zirons as old as 3.8 Ga have been daged from the Wind River Range (Aleinikoff et al. 1989), but rocks older than 2.9 Ga have got to be identifiled in the range. The ca. 2.7 Ga rocks described in this study crop out in the northern portion of the range; the 2.63 Ga Louis Lake batholith has largely obliterated the earlier Archean history in the southern part (Fig. 2).

The major structural feature in the northern Wind River Range is the Mount Helen structural belt (MHSB), a deep-crustal thrust that is up to 5 km wide and extends for nearly 50 km through the center of the range. The belt has a northwest–southeast trend with ~45° dip to the northeast and a top-to-the-southwest sense of shear (Fig. 3). Fragments of the shear zone found in the migmatites of the northern portion of the range indicate that the trend of the structural belt becomes more northerly farther north in the range (Frost et al. 2000*a*). Where the footwall of the MHSB is exposed (1 in Fig. 3), it consists of a granodiorite that is similar in appearance to the Native Lake gneiss of the Washakie terrane (Frost et al. 2006*a*) that makes up the upper plate. The similarity of rock on both sides of the shear zone suggests that the MHSB is an intracrustal structure and that it does not represent a terrane boundary. The MHSB contains numerous boudins of mafic and pelitic granulites (2 in Fig. 3), the margins of which have been retrograded to amphibolite facies (see Frost et al. 2000*a* for details on the metamorphism). Locally within the MHSB are dikes of the ca. 2.67 Ga Bridger granodiorite that have been folded into isoclinal folds (3 in Fig. 3). Dikes and small plutons of Bridger granodiorite also cut the foliation of the MHSB, as does the main Bridger batholith (4 in Fig. 3). In the northern part of the Wind River Range, west of the continental divide, the Bridger batholith intrudes the MHSB, truncating it completely (Fig. 2). These relations, along with the presence of a weak solid-state foliation within the Bridger batholith that is parallel with the trend of the MHSB (5 in Fig. 3), are strong evidence that the MHSB was active during the emplacement of the Bridger batholith (Frost et al. 2000*a*).

Washakie block

The hanging wall of the MHSB contains a suite of gneisses that were termed the Washakie block by Frost et al. (2000*a*). These gneisses have not been intruded by the Bridger batholith, and hence they preserve a record of some of the earlier events in the range. The block consists mainly of tonalitic to granitic gneisses that show varying degrees of migmatization and deformation. Interfolded within the gneisses are packages of supracrustal rocks that are a few hundred metres wide and which may extend for more than a kilometre. These packages include metabasite (possibly metabasalt), sulfidic quartzite, and metapelitic gneiss. Intrusive into these gneisses are a series of mafic dikes. Unlike the dikes in the Owl Creek Mountains, the mafic dikes in the Wind River Range are boudinaged and folded. In most places, they have been metamorphosed, but locally the cores of the larger dikes retain igneous assemblages.

Late Archean granites

The gneisses of the Wind River Range are intruded by undeformed granites of two ages. The older of these is the Louis Lake batholith, which was emplaced at 2630 ± 2 Ma (Frost et al. 1998). The batholith ranges in composition from equigranular granodiorite to porphyritic granite, although minor dioritic and gabbroic phases are present (Frost et al. 2000*b*). In the northwestern portion of its exposure, the batholith is charnockitic with the assemblage Qtz–Pl–Kfs–Bt–Opx ± Aug ± Hbl (abbreviations after Kretz 1983), but over the rest of its range, it is pyroxene-free. Over most of its extent, the batholith is undeformed and carries only a weak magmatic fabric marked by orientation of K-feldspar megacrysts. Locally, near South Pass, gneissic units are present in which the magmatic fabric has been overprinted by later solid-state fabrics.

Although the last major igneous event in the northern part of the Wind River Range was the emplacement of the Bridger batholith, minor magmatic activity continued in this area nearly to the end of the Archean. Frost et al. (1998) report a granodiorite dike from the northernmost limit of the range that was emplaced at 2620 ± 1.5 Ma and that may represent the waning stages of the Louis Lake magmatic event. In addition, the northern portion of the range is intruded by two batholiths that are poorly dated at ca. 2.55 Ga (Stuckless et al. 1985), although the data also permit that these could be part of the magmatic event that produced the Louis Lake batholith.

Teton Range

Archean rocks are exposed over an area that is 50 km long and 16 km wide in the core of the Teton uplift (Fig. 4). Based upon the mapping of Reed (1963, 1973) and our work, we have divided the basement into six units. Four of the units, the Moose Basin gneiss (MBG), layered gneiss, augen gneiss, and Webb Canyon gneiss contain a foliation and hence were emplaced before the latest penetrative deformation. The other two units, the Rendezvous gabbro and the Mount Owen Quartz Monzonite, were emplaced after the last fabric-forming event.

Foliated rocks

The oldest rock unit in the Teton Range is the layered gneiss (Reed 1963, 1973). We recognize several types of layered gneiss in the northern Teton Range. One consists of a suite of pelitic and mafic rocks that locally retain granulite-facies assemblages; others consist of layers that were either igneous rocks or immature sediments. Because the granulite-bearing group is distinctive, we have separated it out and call it the Moose Basin gneiss (MBG); we retain the name layered gneiss for the other gneisses occurring in the rest of the range.

The layered gneiss is a heterogeneous rock consisting of layers of granodioritic gneiss that anastomose around boudins and layers of amphibolite, quartzofeldspathic gneiss, and minor metaperidotite. The rock suite clearly includes orthogneisses ranging in composition from mafic to felsic, but we have

Fig. 4. Geologic map of the Teton Range modified after Reed (1973) showing the location of samples described in this study.

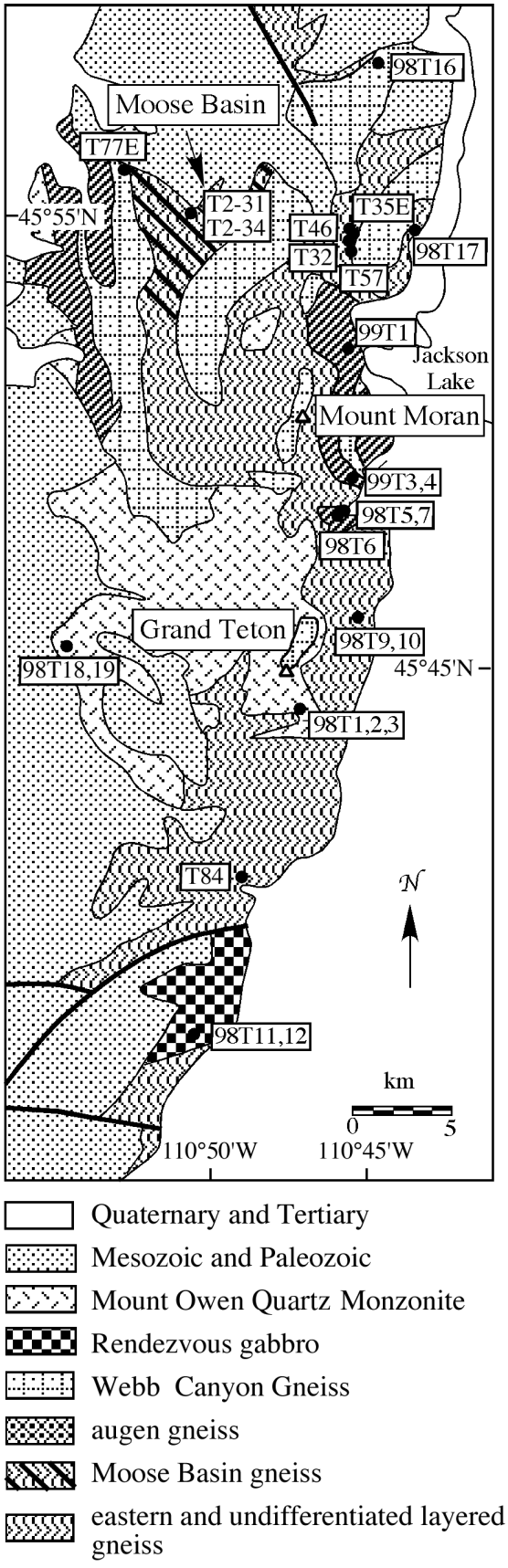

identified Qtz–Bt–Pl schists that we interpret to be metasedimentary horizons. Pelitic rocks are scarce, and consequently it is difficult to determine the metamorphic conditions of the layered gneiss. The rock was clearly subjected to upper amphibolite-facies metamorphism because in many localities it appears to have undergone partial melting.

The MBG consists mostly of interlayered mafic and pelitic rocks with minor leucogranite sills. These pelitic and mafic gneisses are tightly interfolded, which produces the apparent layering of the MBG. The mafic layers of the MBG locally contain relict granulite assemblages (Pl–Opx–Aug ± Grt). The pelitic gneiss contains high-grade assemblage Qtz–Pl–Bt–Ky–Grt (Hildebrandt 1989). These assemblages are indicative of high pressures; Hildebrandt (1989) estimates minimum pressures of 0.8 Gpa. We recognize three folding events in the MBG. The first two were isoclinal folds with axes that are nearly parallel; the third folding event folds the f_1 and f_2 axial planes into an open synform. Most of the fold axes recognized in Moose Basin belong to the f_2 event and most of the layered fabric is parallel to the limbs of these folds. We are uncertain of the southern limit of the MBG and the nature of its contact with the layered gneiss; as a result, we have not drawn a definitive southern contact to this unit on Fig. 4.

Reed (1963, 1973) mapped two foliated orthogneisses in the Teton Range. One is an augen gneiss that forms discontinuous bodies located within the layered gneiss. This rock is a biotite granodiorite that contains relict magmatic K-feldspar megacrysts. The gneiss forms tabular bodies that are concordant with the foliation of the surrounding layered gneiss and carries a foliation that is parallel to that of the surrounding layered gneiss. Preliminary U–Pb zircon data indicate that the augen gneiss can be no older than 2706 Ma (Cornia 2003). Field relations indicates that the augen gneiss is younger than most of the leucosomes in the layered gneiss. However, preliminary dates indicate that a weakly deformed granodiorite sill in the layered gneiss has a minimum age of 2663 Ma (Cornia 2003), indicating that the layered gneiss has a complex magmatic history.

The other orthogneiss in the Teton Range is the Webb Canyon gneiss; this is a strongly foliated leucogranitic orthogneiss that is exposed over much of the northern part of the range. In the Moose Basin area, it occurs in belts that form the western and eastern margins of the MBG (Fig. 4). The contact between the Webb Canyon gneiss and the MBG is parallel to the layering that forms the limbs of the f_2 folds of the MBG (1 in Fig. 5). The main unit of the Webb Canyon gneiss carries a foliation that is parallel to this contact (2 in Fig. 5) but the foliation is not folded. The lineation in this foliation lies parallel to the f_2 folds in the MBG (3 in Fig. 5). The lineation carries an oblique sense of shear that has a sinistral component in the horizontal plane and a thrust sense on the vertical plane. This is particularly well shown by dioritic dikes that were boudinaged during intrusion (4 in Fig. 5). These relations indicate that the Webb Canyon gneiss, which has been dated as 2680 ± 12 Ma (Zartman and Reed 1998), was emplaced during the f_2 folding event.

Post-tectonic magmatic rocks

The Rendezvous gabbro is a hornblende gabbro that has no penetrative deformation and that preserves a primary ig-

Fig. 5. Block diagram showing relations between the layered gneiss in Moose Basin and the Webb Canyon gneiss. Width of block is about 1 km. Key relations are (1) the contact between the two units is parallel to the limbs of the f_2 folds in the layered gneiss, (2) foliation in the Webb Canyon gneiss is parallel to the between the two units, (3) lineation in the Webb Canyon gneiss is parallel to the f_2 fold axes in the layered gneiss, and (4) dioritic dikes in the Webb Canyon gneiss are boudinaged with sinistral sense of shear on horizontal surfaces and thrust sense on vertical surfaces, consistent with sense of shear on the lineation in the Moose Basin gneiss.

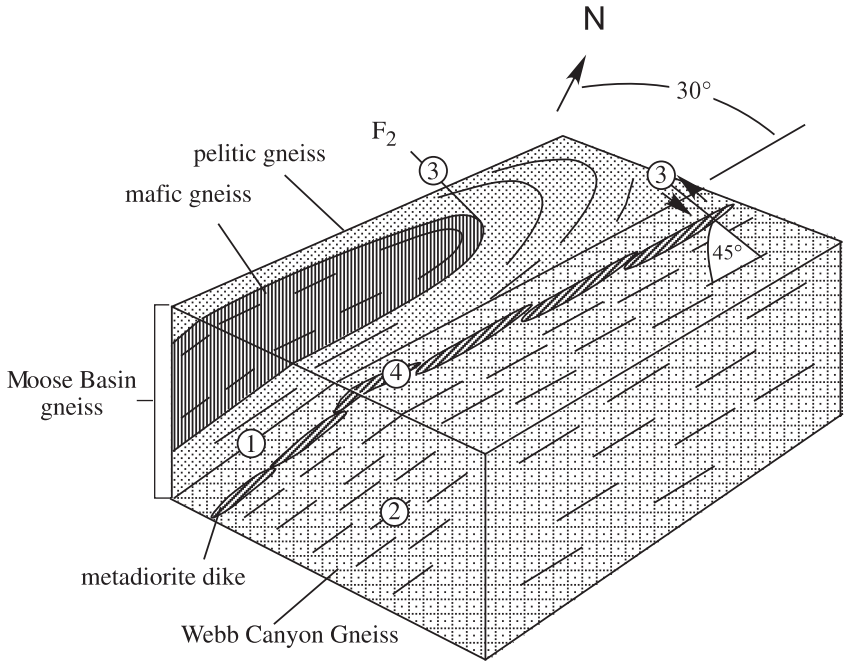

neous fabric. The northern contact is fault bounded, and Reed and Houston (1993) argue that the gabbro clearly truncates the foliation of the layered gneiss along its southern boundary. The other late igneous body is the Mount Owen Quartz Monzonite. The intrusion is a muscovite-bearing and locally garnet-bearing leucogranite that is texturally heterogeneous, with pegmatitic and fine-grained zones grading into each other on a metre scale. The Mount Owen Quartz Monzonite was intruded into the center of the range at 2547 ± 3 Ma (Zartman and Reed 1998) and truncates all foliations. The last Precambrian igneous event in the range was the emplacement of a series of east–west-trending mafic dikes, one of which yielded an Ar–Ar hornblende date of 769 ± 5 Ma (Harlan et al. 1997).

U–Pb zircon and baddeleyite geochronology

To constrain the timing of deformation in the western Owl Creek Mountains, Wind River Range, and Teton Range, we have obtained U–Pb ages of zircon and baddeleyite from tholeiitic dikes in the western Owl Creek Mountains and zircon from tholeiitic dikes in the Wind River Range, the syntectonic Webb Canyon gneiss (98T17), and the post-tectonic Rendezvous gabbro (98T12) (Table 1).

Tholeiitic dike from the eastern Wind River Range (sample 95Bob20)

The tholeiitic dike sampled for geochronology is about 5 m wide and occurs as folded boudins. The margins of the boudins have been metamorphosed to amphibolite facies assemblages but the cores of the boudins retain the magmatic assemblage of Pl–Opx–Aug. Zircon from this rock occurs as skeletal striated grains typical of magmatic growth in mafic rocks. A regression of U–Pb data from five multigrain analyses has a good linear fit (mean square of the weighted deviation (MSWD) = 1.8) and an upper intercept of 2681.3 ± 1.7 Ma (Table 1) that we interpret as the crystallization age of this dike (Fig. 6A).

Tholeiitic dike from the western Owl Creek Mountains (sample 98OC-15a)

A coarse-grained core of one of the widest dikes (ca. 10 m) in the western Owl Creek Mountains was sampled for U–Pb baddeleyite dating. This sample contains primary plagioclase, orthopyroxene, and augite, as well as small amounts of secondary hornblende and quartz. The rock contains both zircon and baddeleyite. Two morphologies of baddeleyite occur in the dike: one is clear and the other is mottled. Heaman and LeCheminant (1993) attribute the mottled appearance to polycrystalline growth of zircon on the baddeleyite during metamorphism.

Five fractions of baddeleyite and one fraction of zircon were analyzed from this sample. Two clear fractions of baddeleyite give an upper intercept age of 2682.7 ± 7.5 Ma; one of these fractions is concordant with an age of 2681.7 ± 4.9 Ma (Table 1, Fig 6B). A single zircon yielded a $^{207}Pb/^{206}Pb$ date of 2864 ± 2 Ma and is interpreted as being xenocrystic. The mottled baddeleyite fractions give younger ages that we interpret as mixtures between magmatic growth and younger zircon overgrowths during minor greenschist alteration that has affected the rock. This interpretation is supported by a crude correlation between radiogenic $^{206}Pb/^{208}Pb$ (related to U/Th of minerals) and degree of mottling, discordance, and $^{207}Pb/^{206}Pb$ dates (Table 1). Purest baddeleyite grains have

Fig. 6. Concordia diagrams: (A) Zircon data from tholeiitic dike from the Wind River Range (sample 95Bob20), (B) baddeleyite data from tholeiitic dike from the Owl Creek Mountains (sample 98OC12), (C) zircon data from the Webb Canyon gneiss (sample 98T-17), (D) magmatic zircon data from the Rendezvous gabbro (sample 98-T12). Shaded ellipses were used in the regression. MSWD, mean square of the weighted deviation.

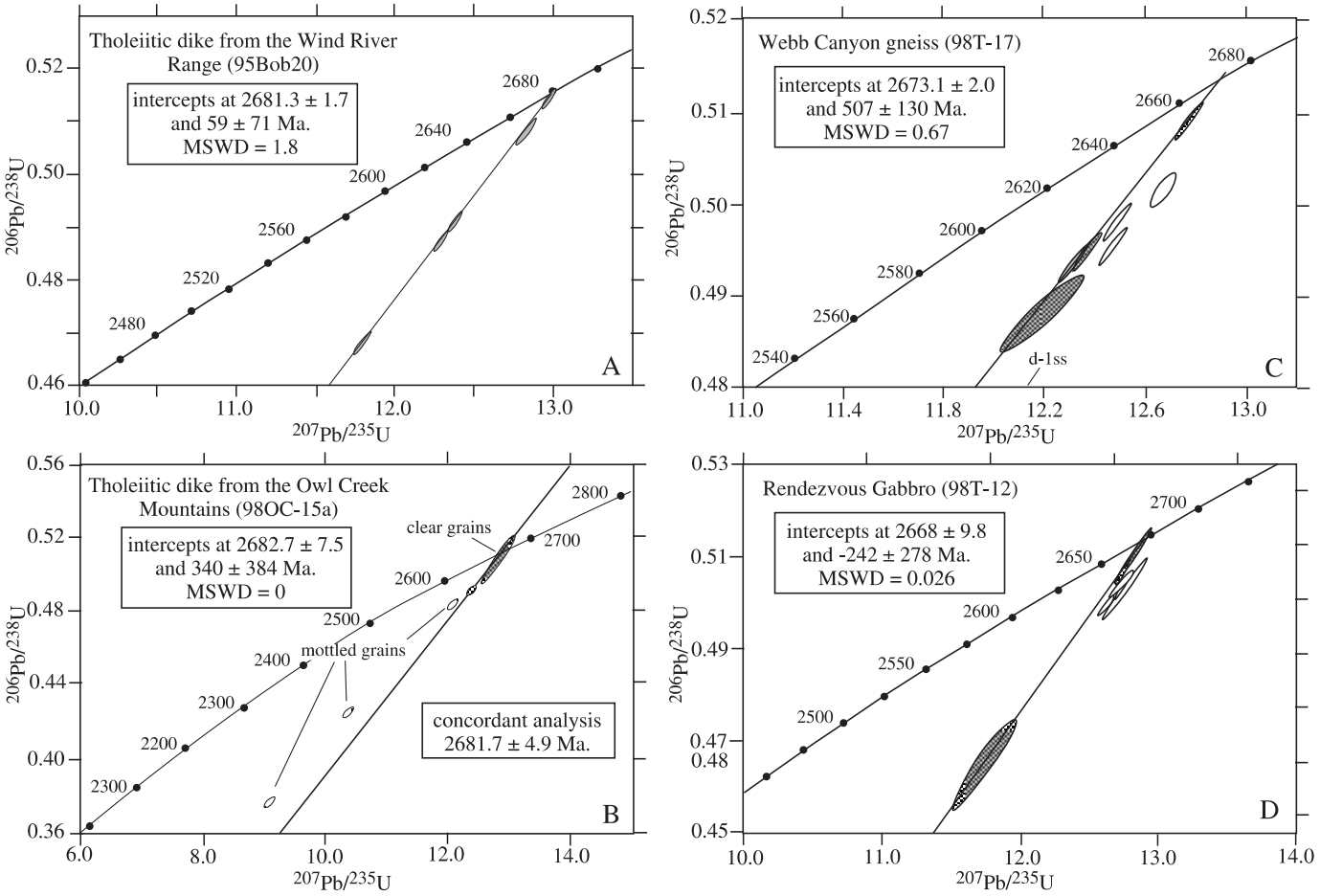

the highest $^{206}Pb/^{208}Pb$, consistent with lower Th/U relative to zircon.

Webb Canyon gneiss (sample 98T-17)

Zircon from sample 98T-17 includes four distinct morphologies. One morphology consists of rounded, short, stubby, brown grains. Grains of the second morphology are similarly rounded but have a higher aspect ratio than those in the first morphology. Zircons of the third morphology are short, honey-colored, and doubly terminated. Those of the fourth morphology are long, slender, honey-colored, and doubly terminated. Four fractions of the third morphology and four fractions of the fourth morphology were selected for air abrasion and dissolution because they showed oscillatory zoning in cathodoluminescence (Cornia 2003). Initial Pb isotopic compositions for this sample were determined from the Pb isotopic composition of step-dissolved, coexisting alkali feldspar. This sample is unusual in that the feldspar values are very radiogenic ($^{206}Pb/^{204}Pb$ = 32.19, Table 1 note). The U concentrations of zircon are relatively high, however, with high radiogenic to common Pb ($^{206}Pb/^{204}Pb$), so that correcting the data with less radiogenic compositions, such as the Stacey and Kramers (1975) model, has little to no effect on the concordia coordinates and ages.

The Pb and U concentrations for zircon grains from the two morphologies overlap, and no correlation exists among morphology, U or Pb concentrations, percent discordance, or radiogenic $^{206}Pb/^{208}Pb$ values (Table 1). This leads us to conclude that both morphologies grew from the same magma or from magmas with similar U–Pb characteristics. The resulting data define a relatively tight cluster (Fig 6C) with data from all seven air-abraded fractions being <6% discordant. This cluster is interpreted as representing dominantly magmatic growth with a slight amount of inheritance. A minimum estimate for the magmatic age of the Webb Canyon gneiss comes from the four fractions with the least evidence of inheritance. A regression through these four points yields an upper intercept of 2673.1 ± 2 Ma and a lower intercept of 507 ± 130 Ma (MSWD = 0.67). This age is within error of the age of the Webb Canyon gneiss reported in Zartman and Reed (1998) of 2680 ± 12 Ma.

Rendezvous gabbro (sample 98T-12)

Zircon grains from this sample display two morphologies. One morphology consists of slightly rounded, long, slender, and honey-colored grains. The second consists of brown, pear-shaped grains. Both morphologies are clear in plain light and do not display obvious cores. Seven fractions of

Table 1. U–Pb thermal ionization mass spectrometry data.

Sample	Weight (μg)	U (ppm)	Tot Pb (ppm)	Com Pb (ppm)	Corrected atomic ratios $\frac{^{206}Pb}{^{204}Pb}$	$\frac{^{206}Pb}{^{208}Pb}$	$\frac{^{206}Pb}{^{238}U}$ (rad.)
Washakie block, Wind River Range							
95BOB-20 mafic dike (UTM S12 062488E, 478186N)							
nm1 sk-str dk pk 5g aa2	13.90	129	78	0.31	11823	5.62	0.5147
nm1 sk-str pk 12g aa3	9.28	85	51	0.32	7497	6.04	0.5105
nm1 sk-str dk pk 6g	11.10	91	53	0.52	4853	6.05	0.4931
nm1 sk-str dk pk 5g aa	13.90	83	48	0.09	24387	5.72	0.4896
nm3 sk-str dk pk 4g	11.10	117	64	0.57	5317	6.74	0.4703
Western Owl Creek Mountains							
980c-15A mafic dike (UTM S12 068762E, 482666N)							
nm1.4a clr badd 1gr*	1.12	88	47	0.46	5483	52.51	0.5122
nm1.4a clr badd 3gr*	2.33	342	175	1.92	4920	110.64	0.4944
nm1.4a mot badd B 1gr	3.16	509	261	6.51	2128	61.90	0.4862
nm1.4a mot badd A 1gr	5.60	98	49	0.26	8992	5.49	0.4254
nm1.4a mot badd 3gr	3.72	1217	581	85.23	315	12.77	0.3785
zircon euh 1gr	3.65	316	185	14.79	563	6.70	0.4622
Teton Range							
Webb Canyon gneiss (98T-17) (UTM 052215E, 486211N)							
nm2 1s aa (mor 4) 8gr*	11.60	429	248	1.04	19124	7.50	0.5081
d-1 ss aa (mor 3) 4gr	12.30	304	175	1.07	13069	6.99	0.5024
nm3 1s aa (mor 4) 9gr	11.60	710	404	1.81	17772	7.08	0.4977
nm1 1s aa (mor 4) 12gr*	16.70	330	184	1.62	9205	8.31	0.4947
nm3 ss aa (mor 3) 3gr*	9.28	454	251	2.08	9817	8.99	0.4928
D-1 1s aa (mor 4) 8gr	17.80	306	172	0.48	28945	7.52	0.4954
nm1 ss aa (mor 3) 4gr*	7.43	116	64	0.39	13336	7.81	0.4887
D-1 ss (mor 3) 10gr	23.00	879	445	0.08	427856	7.87	0.4499
Rendezvous gabbro (98T-12) (UTM S12 051262E, 482714N)							
d-1 1s aa 2gr*	5.57	48	31	1.33	1056	5.12	0.5113
nm1 pear aa 8gr*	8.35	128	77	7.26	519	14.48	0.5071
d-2 pear aa 8gr	23.20	294	163	2.71	3090	13.31	0.5037
d-2 1s 4gr	26.00	312	175	0.06	136529	8.99	0.5030
d-1 1s 9gr	11.10	245	148	8.89	791	7.91	0.5028
d-2 pear 4gr	32.50	303	161	0.76	11238	21.80	0.4990
d-3 pear aa 2gr*	4.22	48	29	4.24	311	8.65	0.4658

Note: Corrected atomic ratios: $^{206}Pb/^{204}Pb$ corrected for blank and mass discrimination; all others corrected for blank, mass discrimination, and initial for laboratory blank of 15–5 pg Pb; com Pb, initial common Pb corrected for laboratory blank of 15–5 pg Pb for zircon; rad, radiogenic; % Disc., percent d-_ and nm_, angles of diamagnetic and paramagnetic susceptibility on a barrier style Frantz separator, respectively; sk-str, skeletal, striated; clr badd, clear number of grains if <40; aa, air abraded; aa_ and p_, numerical identifier if picks are similar in all other ways; *, used for regression. Analytical details: Zircon with a mixed $^{208}Pb/^{235}U$ tracer. Pb and U samples were loaded onto single rhenium filaments with silica gel and graphite, respectively. Isotopic compositions collector if the $^{206}Pb/^{204}Pb$ was >200; all other isotopes were measured in Faraday collectors. Mass discrimination factors of 0.132–0.048 ± 0.06 %/amu respectively. Procedural blanks improved from 15 to 5 pg Pb during the course of the study. Isotopic composition of the Pb blank was estimated as 19.09 ± intercepts, and uncertainties were calculated using PBDAT and ISOPLOT programs (Ludwig 1988, 1991). Initial Pb isotopic compositions were estimated (used granodiorite 98OC-6 13.970, 15.094, 34.314, Kirkwood 2000), Webb Canyon 98T-17 (used 32.192, 20.527, 51.532, Cornia 2003), Rendezvous gabbro $^{206}Pb/^{204}Pb$, $^{207}Pb/^{204}Pb$, and $^{208}Pb/^{204}Pb$, respectively. The decay constants used by PBDAT are those recommended by the International Union of Geological 137.88. $^{208}Pb/^{235}U$ tracer was calibrated against MIT2 gravimetric standard and yielded a $^{206}Pb/^{238}U$ date of 419.26 ± 0.64 Ma for zircon standard R33

zircon were analyzed, with five of those fractions being air abraded to remove any later overgrowths or metamict rims that may be present. Initial Pb isotopic compositions were determined from the isotopic composition of plagioclase from this sample. There is no correlation among morphology, U or Pb concentrations, percent discordance, or $^{206}Pb/^{208}Pb$ values (Table 1), so both morphologies are interpreted to have grown from the same magma or from magmas with similar U–Pb–Th compositions.

The data from the seven points form two tight clusters near concordia; one point overlaps concordia, one point is 10% discordant, and the rest are <4% discordant (Fig. 6D).

Corrected atomic ratios									
% Error	$^{207}Pb/^{235}U$ (rad.)	% Error	$^{207}Pb/^{206}Pb$ (rad.)	% Error	$^{206}Pb/^{238}U$ age (Ma)	$^{207}Pb/^{235}U$ age (Ma)	$^{207}Pb/^{206}Pb$ age (Ma)	Rho	% Disc.
Crystallization age = 2681.3 ± 1.7 Ma (MSWD = 1.8) five-point chord									
(0.34)	12.9931	(0.34)	0.1831	(0.05)	2677	2679	2680.9±0.9	0.99	0.2
(0.39)	12.8962	(0.37)	0.1832	(0.11)	2659	2672	2682.1±1.8	0.96	1.1
(0.37)	12.4384	(0.35)	0.1829	(0.08)	2584	2638	2679.6±1.4	0.97	4.3
(0.35)	12.3594	(0.35)	0.1831	(0.08)	2569	2632	2681.2±1.3	0.98	5.1
(0.33)	11.8586	(0.34)	0.1829	(0.05)	2485	2593	2679.0±0.9	0.99	8.7
Crystallization age = 2682.7 ± 7.5 Ma (MSWD = 0) two-point chord*									
(1.62)	12.9360	(1.59)	0.1832	(0.29)	2666	2675	2681.7±4.9	0.98	0.7
(0.46)	12.4474	(0.43)	0.1826	(0.14)	2590	2639	2676.7±2.3	0.95	3.9
(0.36)	12.0959	(0.35)	0.1805	(0.08)	2554	2612	2657.0±1.4	0.97	4.7
(0.60)	10.3684	(0.53)	0.1768	(0.23)	2285	2468	2622.8±3.9	0.92	15.3
(0.33)	9.0967	(0.34)	0.1743	(0.10)	2069	2348	2599.3±1.7	0.96	23.8
(0.38)	13.0416	(0.37)	0.2047	(0.09)	2449	2683	2863.7±1.5	0.97	17.4
Crystallization age = 2673.1 ± 2 Ma (MSWD = 0.67) four-point regression*									
(0.34)	12.7471	(0.35)	0.1819	(0.07)	2649	2661	2670.7±1.1	0.98	1.0
(0.37)	12.6562	(0.39)	0.1827	(0.11)	2624	2654	2677.5±1.7	0.96	2.4
(0.37)	12.4865	(0.39)	0.1820	(0.08)	2604	2642	2671.0±1.3	0.98	3.1
(0.37)	12.3653	(0.41)	0.1813	(0.12)	2591	2633	2664.6±2.0	0.96	3.4
(0.35)	12.3099	(0.41)	0.1812	(0.13)	2583	2628	2663.6±2.2	0.95	3.7
(0.37)	12.4744	(0.41)	0.1826	(0.12)	2594	2641	2676.7±2.0	0.96	3.7
(0.71)	12.2340	(1.30)	0.1816	(0.64)	2565	2623	2667.3±11.0	0.97	4.6
(0.43)	11.2453	(0.44)	0.1813	(0.08)	2395	2544	2664.6±1.4	0.98	12.1
Crystallization age = 2668 ± 9.8 Ga (MSWD = 0.03) three-point regression*									
(0.75)	12.8357	(0.73)	0.1821	(0.23)	2662	2668	2671.9±3.8	0.95	0.5
(0.39)	12.7346	(0.38)	0.1821	(0.12)	2644	2660	2672.3±2.0	0.95	1.3
(0.55)	12.7235	(0.57)	0.1832	(0.16)	2630	2659	2682.0±2.6	0.96	2.4
(0.39)	12.7214	(0.40)	0.1834	(0.08)	2627	2659	2684.1±1.4	0.98	2.6
(1.03)	12.7522	(1.05)	0.1840	(0.18)	2626	2662	2688.9±3.0	0.98	2.9
(0.36)	12.6034	(0.37)	0.1832	(0.10)	2610	2650	2681.9±1.6	0.97	3.3
(1.60)	11.7527	(1.53)	0.1830	(0.54)	2465	2585	2680.1±8.9	0.94	9.6

Pb; values in parentheses are 2σ errors in percent. Rho, $^{206}Pb/^{238}U$ vs. $^{207}Pb/^{235}U$ error correlation coefficient; tot Pb, radiogenic + initial common Pb corrected discordant; UTM (Universal Transverse Mercator) coordinates refer to North American Datum (NAD) 27; MSWD, mean square of the weighted deviation; baddeleyite; mot badd, mottled baddeleyite; ss, short and stubby; ls, elongate; pear, facetted and squat; dk pk, dark pink; br, brown; yw, yellow; _gr, dissolution and chemistry were adapted from methods developed by Krogh (1973) and Parrish et al. (1987). Aliquots of dissolved sample were spiked were measured in multi-collector, static mode on a VG Sector mass spectrometer at the University of Wyoming, Laramie, with ^{204}Pb in a Daly-photomultiplier (atomic mass units) for Pb, depending on silica gel batch, and 0.0 ± 0.06%/amu for U were determined by replicate analyses of NIST SRM 981 and U-500, 0.5, 15.652 ± 0.2, and 38.81 ± 0.2 for $^{206}Pb/^{204}Pb$, $^{207}Pb/^{204}Pb$, and $^{208}Pb/^{204}Pb$, respectively. U blanks were consistently <1 pg. Concordia coordinates, by measured feldspars: 95BOB-20 (used feldspar compositions from the Native Lake gneiss 14.186, 15.094, 33.876: 6/4, 7/4, 8/4, Frost et al. 1998), 98OC-15A 98T-12 (used 14.713, 15.238, 34.040, Cornia 2003). Uncertainties on the measured feldspar Pb isotopic compositions were ± 0.12%, 0.18%, and 0.24% for Sciences Subcommission on Geochronology (Steiger and Jäger 1977): 0.155125×10^{-9}/year for ^{238}U, 0.98485×10^{-9}/year for ^{235}U and present-day $^{238}U/^{235}U$ = ($^{207}Pb/^{235}U$ date of 420.11 ± 0.59 Ma), in good agreement with the Royal Ontario Museum (ROM) date for R33 (Black et al. 2004).

The non-linear scatter of the data is slight; $^{207}Pb/^{206}Pb$ ages range from 2672 to 2689 Ma. We interpret the scatter to be caused by small amounts of inheritance. The best estimate for the magmatic age of the Rendezvous gabbro comes from a regression through three points with the least evidence for inheritance. This produces a chord with an upper intercept of 2668 ± 9.8 Ma and a lower intercept of 242 ± 278 Ma (MSWD = 0.03). The four points not included in the regression lie to the right of the chord and are interpreted to contain varying degrees of inheritance: this interpretation is supported by the higher U and Pb concentrations in these fractions than in the three that were used for the regression.

Table 2. Whole-rock analyses of rocks from the Teton Range.

	Layered gneiss					Augen gneiss		Webb Canyon gneiss		Mount Owen Quartz Monzonite							
Sample:	98T-6	98T-7	98T-8	98T-9	99T-1	99T-6	99-T4	98T-16	98T-17	98T-1	98T-2	98T-3	98T-5	98T-10	98T-18	98T-19	99T-5
SiO_2 (wt.%)	71.9	74	71	71.7	69.5	69.1	71.4	76.2	79.4	73.9	75.4	70.7	72.9	74.1	74.7	74.9	73.9
TiO_2	0.28	0.29	0.95	0.35	0.44	0.45	0.37	0.19	0.11	0.04	0.02	0.34	0.13	0.19	0.07	0.09	0.15
Al_2O_3	13.6	13.4	11.8	14.5	15.5	14.9	14.2	10.4	10.8	14.2	14.5	14.4	13.8	13.7	13.5	13.7	13.8
$Fe_2O_3^T$	3.2	2.77	6.21	3.05	3.63	3.06	2.72	4.08	2.73	0.95	0.87	3.61	1.29	1.68	1.5	1.46	1.23
MnO	0.04	0.03	0.06	0.03	0.04	0.03	0.03	0.05	0.02	0.02	0	0.05	0	0.01	0.01	0	0
MgO	0.51	1.17	1.68	0.79	0.87	1.19	1.02	0.06	0.1	0.14	0.1	0.78	0.36	0.37	0.2	0.27	0.33
CaO	3.17	2.36	2.34	3.43	4.51	2.72	2.46	1.46	0.76	0.92	0.65	3.54	1.41	1.14	0.85	0.87	1.43
Na_2O	3.52	3.83	2.64	4	3.55	3.81	3.65	3.36	3.98	4.06	3.65	3.94	3.31	3.15	3.17	3.09	2.87
K_2O	2.11	1.92	2.14	1.23	1.32	3.29	3.34	2.79	2.37	4.76	4.31	1.35	5.29	5.33	5.34	5.56	5.18
P_2O_5	0.06	0.05	0.28	0.08	0.12	0.12	0.11	0.01	0	0.05	0.06	0.08	0.05	0.06	0.07	0.06	0.05
LOI	0.3	0.2	0.2	0.35	0.65	0.35	0.15	0.15	0.1	0.2	0.5	0.15	0.25	0.4	0.3	0.35	0.8
Total	98.69	100.02	99.30	99.51	100.13	99.02	99.45	98.75	100.37	99.24	100.06	98.94	98.79	100.13	99.71	100.35	99.74
MALI	2.46	3.39	2.44	1.8	0.36	4.38	4.53	4.69	5.59	7.9	7.31	1.75	7.19	7.34	7.66	7.78	6.62
Fe*	0.86	0.7	0.79	0.79	0.81	0.72	0.73	0.99	0.96	0.87	0.9	0.82	0.78	0.82	0.88	0.84	0.79
ASI	0.993	1.068	1.152	1.039	1.021	1.029	1.027	0.93	1.029	1.061	1.239	1.015	1.014	1.064	1.091	1.093	1.077
Trace elements (ppm)																	
Y	34	120	152	27	28	18	13	275	156	35	19	66	25	35	37	58	29
Rb	64	100	102	71	45	98	103	41	37	149	130	66	181	179	270	197	165
Sr	123	71	112	172	211	188	172	96	35	33	13	131	67	70	36	56	100
Ba	637	646	666	536	499	812	653	1220	350	321	0	345	695	737	274	539	750
Zr	257	302	593	307	269	217	182	508	402	70	40	271	118	163	99	113	148
Nb	22	24	35	14	12	10	48	13	38	17	17	20	11	14	18	16	10
Th	50			37.2	19.6	36.4	20.5		18.3	15.4		24.2				24.2	59
U	4			3.2	3.5	2.7	1.2		3.3	4.4		4.2				4.8	5.6

Note: $Fe_2O_3^T$, total iron content shown as Fe_2O_3; LOI, loss on ignition; MALI, modified alkali-lime index; ASI, aluminum saturation index; Fe*, $(Fe_2O_3^T \times 0.9)/[(Fe_2O_3^T \times 0.9) + MgO)]$.

Fig. 7. Granite classification diagrams of Frost et al. (2001) showing the compositional ranges of ca. 2.7 Ga granitoids from the Wind River and Teton ranges: (A) ASI, aluminum saturation index; (B) Fe*, $(Fe_2O_3^T \times 0.9)/[(Fe_2O_3^T \times 0.9) + MgO)]$; (C) MALI, modified alkali-lime index. Field for the Webb Canyon gneiss includes 15 analyses reported in Barker et al. (1979) and Miller et al. (1986). Field for granodioritic orthogneiss includes seven analyses from Miller et al. (1986). Field for the Bridger batholith from Frost et al. (1998).

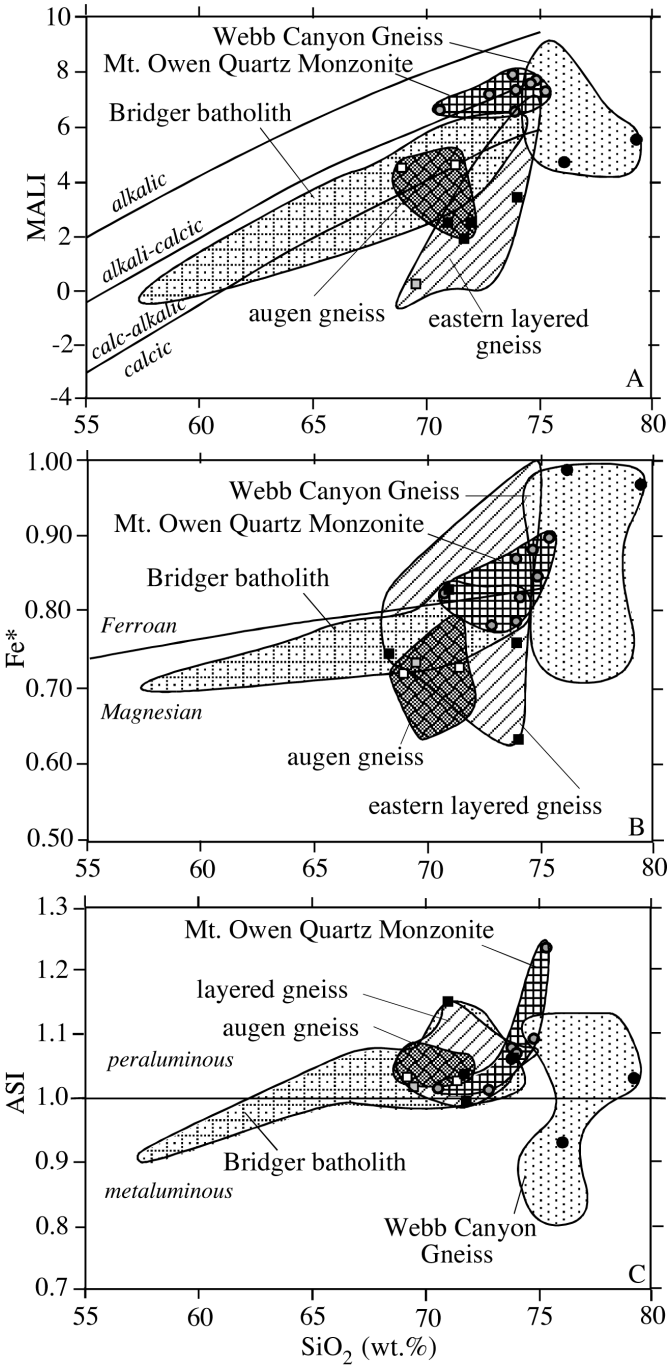

Fig. 8. AFM (alkalis–Fe_2O_3–MgO) diagram comparing composition of the Rendezvous gabbro, amphibolites from the eastern layered gneiss, and dikes from the western Owl Creek Mountains. Field for amphibolites from the layered gneiss includes 10 analyses from Miller et al. (1986).

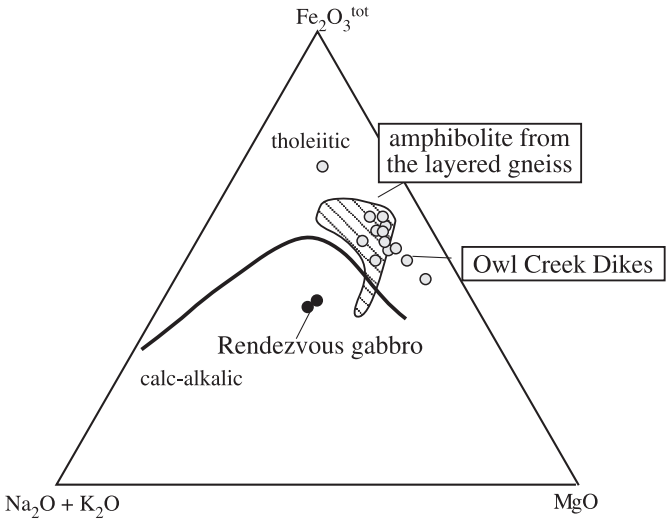

Whole-rock geochemistry

New geochemical analyses for rocks from the Teton Range, as well as tholeiitic dikes in the Owl Creek Mountains, are given in Tables 2 and 3. These analyses are shown as points in Figs. 7–9. Other analyses obtained on the Precambrian rocks of the Teton Range were reported in Miller et al. (1986) and Barker et al. (1979) and are shown as fields in these figures.

Major elements

The four felsic rock types from the Teton Range have a more restricted range of silica content than does the Bridger batholith from the Wind River Range (Fig. 7). The augen gneiss is a weakly peraluminous, magnesian granitoid that overlaps the compositional range of the Bridger batholith, but it extends to more calcic and magnesian compositions. The felsic portions of the layered gneiss cover a wide compositional range. These rocks likely represent a mixture of orthogneisses and paragneisses, and thus their chemical spread reflects sedimentary (and possibly metamorphic), as well as igneous processes. One sample, 98T8, clearly has a sedimentary protolith, based upon its high quartz content, which makes up >60% of the rock. This explains its low Al_2O_3 compared with other samples of the layered gneiss, as well as its high P_2O_5 content. The Mount Owen Quartz Monzonite ranges from weakly to strongly peraluminous and bridges the calc-alkalic–alkali-calcic and magnesian–ferroan fields.

The high silica content of the Webb Canyon gneiss makes it compositionally distinct from the other felsic rocks of the Teton Range. The Webb Canyon gneiss is a leucogranite (i.e., >75 wt.% SiO_2), and like most leucogranites it has a highly variable modified alkali-lime index (MALI) and Fe*, $(Fe_2O_3^T \times 0.9)/[(Fe_2O_3^T \times 0.9) + MgO)]$ (Frost et al. 2001). It ranges from calcic to alkali-calcic (Fig. 7A) and from magnesian to ferroan (Fig. 7B). Unlike the peraluminous

Fig. 9. (A) Plot of Zr vs. silica and (B) plot of Rb/Sr vs. Zr for the Webb Canyon gneiss (includes two points reported in Miller et al. (1986)), the augen gneiss, and the Mount Owen Quartz Monzonite. Composition ranges for the Bridger batholith from Frost et al. (1998).

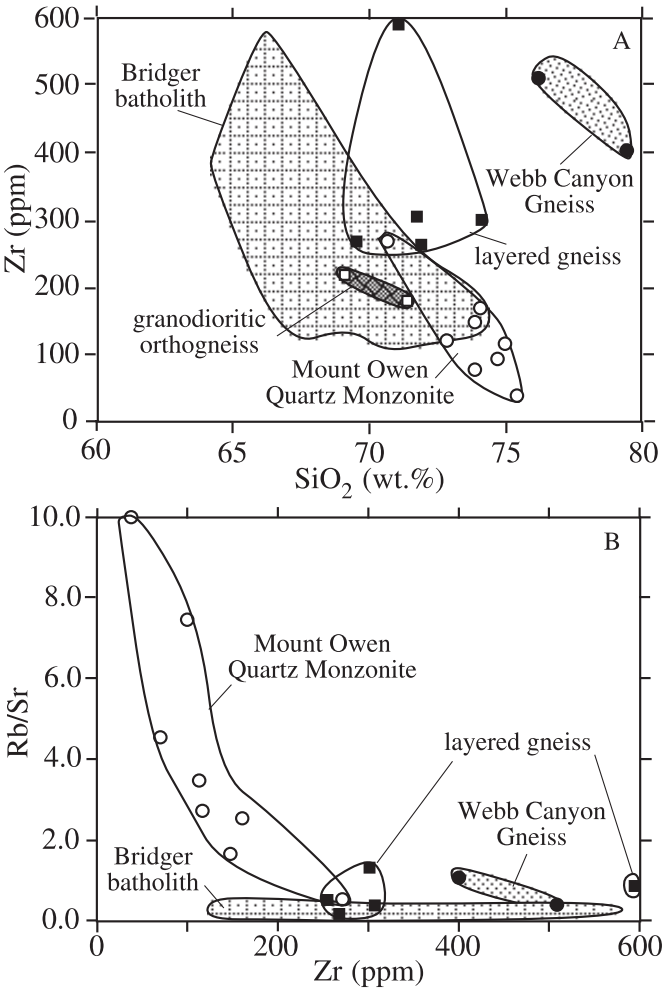

leucogranites described by Frost et al. (2001), the Webb Canyon gneiss is not strongly peraluminous and many samples are metaluminous (Fig. 7C).

All of the granitoids in the Teton Range are moderately sodic with Na_2O abundances ranging from 3 to 5 wt.%, and some samples of the Webb Canyon gneiss have as much as 6 wt.% Na_2O. Potassium is far more variable; within single suites K_2O varying from near 1 to >5 wt.%.

The mafic dikes from the Owl Creek Mountains are tholeiitic and evince a strong iron-enrichment trend (Fig. 8). Our single amphibolite analyzed from the layered gneiss also is tholeiitic, as are most of the amphibolites analyzed by Miller et al. (1986). In contrast, the two samples of the Rendezvous gabbro are calc-alkalic and are compositionally distinct from the amphibolites in the layered gneiss.

Trace elements

The Bridger batholith and other felsic rocks of the Teton Range show a marked decrease in Zr content with increasing SiO_2 (Fig. 9A). The Zr content of a granitic melt is a function of its temperature and melt composition (Watson and Harrison 1983). The pattern of Zr content of the Bridger batholith and Mount Owen Quartz Monzonite samples behaves similarly to most granites. It falls steeply with increasing silica because Zr becomes strongly compatible once zircon begins to crystallize. The layered gneiss has somewhat elevated Zr for given silica and plots between the Webb Canyon gneiss and the Bridger batholith. Because the layered gneiss could be either an orthogneiss or a paragneiss, we are uncertain about the significance of its Zr content. Certainly, the sample with the highest Zr (sample 98T8) is a paragneiss; the high Zr content reflects detrital zircon. Compared with the other rocks, the samples of Webb Canyon gneiss have a much higher Zr content for their SiO_2 content.

Because Zr behaves incompatibly in these high-Si rocks, we can use it as a monitor for differentiation (Fig. 9B). Rb/Sr shows only minimal variation with respect to Zr for the Bridger batholith, layered gneiss, and Webb Canyon gneiss, but in the Mount Owen Quartz Monzonite it shows a dramatic increase with falling Zr. This suggests that much of the chemical variation in the Mount Owen Quartz Monzonite is owing to fractional crystallization of plagioclase and zircon. The strong increase in the aluminum saturation index (ASI) with increasing silica (Fig. 7C) for the Mount Owen Quartz Monzonite suggests that Al-rich phases (muscovite and garnet) did not crystallize until late in the history of the magma.

The Webb Canyon gneiss has much higher rare-earth element (REE) contents and a flatter REE pattern than the Bridger batholith or other felsic rocks from the Teton Range (Table 4; Fig. 10). The Bridger batholith has a REE pattern that is typical of other granodioritic batholiths, with a distinct depletion in heavy REEs and small to non-existant Eu anomaly (Frost et al. 1998). The other granitic rocks from the Teton Range, the augen gneiss, and layered gneiss, have similar patterns to the Bridger batholith but with somewhat more pronounced negative Eu anomalies. The REE pattern of the Mount Owen Quartz Monzonite also has a distinct negative europium anomaly, Eu/Eu* for the Mount Owen Quartz Monzonite increases with increasing silica content, consistent with the contention that plagioclase fractionation plays an important role in the differentiation of this pluton.

Isotope geology

In this paper, we present 28 Nd and Sr and 18 Pb isotopic analyses from the Teton Range along with samples of mafic dikes from the Wind River Range and Owl Creek Mountains (Tables 5, 6). Included in the analyses from the Teton Range are 12 samples collected by Miller et al. (1986), the locations of which are shown in Fig. 4.

Several key observations can be made from the Nd isotopic compositions of the rocks in Table 5. First the initial Nd isotopic compositions of the MBG are distinct from those of the layered gneiss (Fig. 11). Because we do not know the formation age for the layered gneiss, for comparison we have calculated the initial ε_{Nd} for both gneisses at 2700 Ma. The initial ε_{Nd} values for the four samples of MBG are negative whereas those for the nine samples of layered gneiss are mostly positive. Significantly, the single sample of the layered gneiss that we can confidently identify as metasediment (sample 98T8) has the most radiogenic Nd isotopic composition.

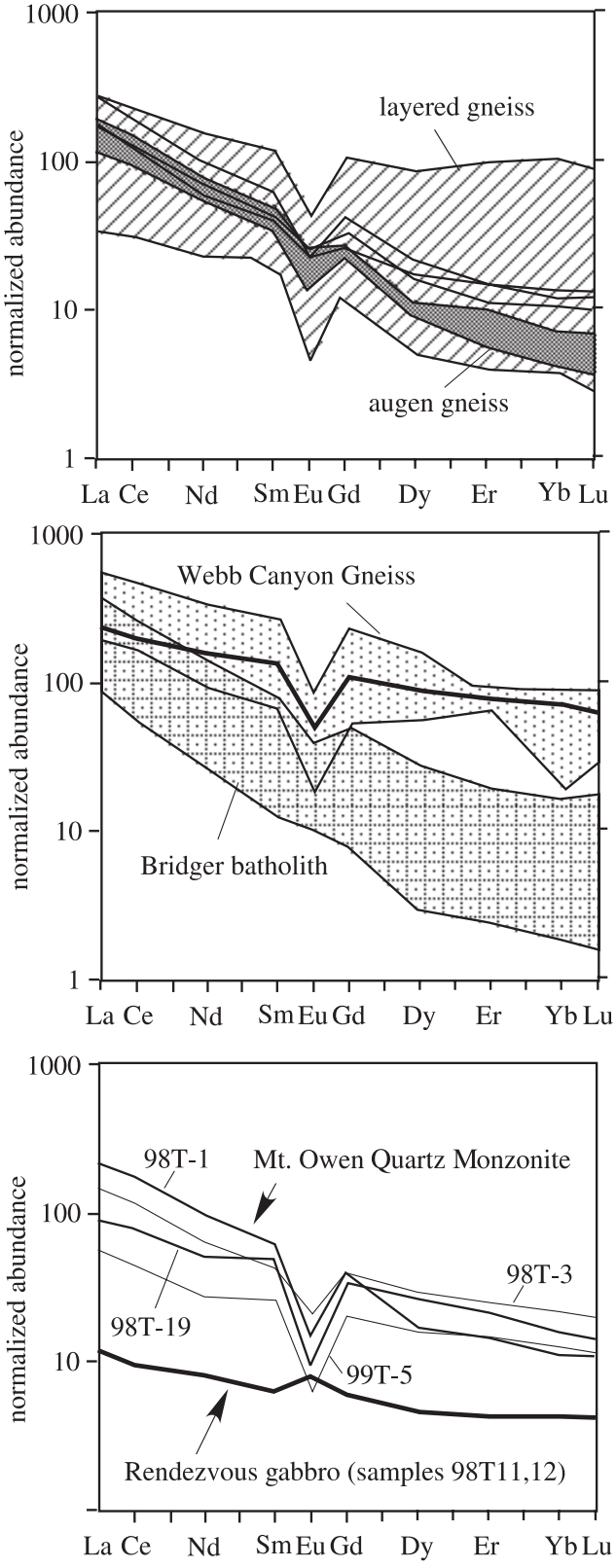

Fig. 10. Chondrite-normalized rare-earth element abundances for (A) layered gneiss and augen gneiss from the Teton Range, (B) Webb Canyon gneiss and Bridger batholiths, (C) Mount Owen Quartz Monzonite and the Rendezvous gabbro. Field for Webb Canyon gneiss includes six analyses reported in Barker et al. (1979) and Miller et al. (1986). Field for the Bridger batholith is from Frost et al. (1998). Normalizing factors come from Wakita et al. (1971).

Figure 11 also shows that the Webb Canyon gneiss, whose chemistry indicates that it is a crustal melt, could have been generated from rocks with the isotopic composition of the layered gneiss, but not from the samples of the MBG that we measured. In contrast, the Mount Owen Quartz Monzonite has an isotopic composition that could have been derived either from the most evolved samples of the layered gneiss or from the most primitive samples of the MBG or from some combination. Nd isotopic compositions of the Rendezvous gabbro and the tholeiitic dikes from the Wind River Range and the western Owl Creek Mountains are consistent with mantle melts that have undergone about 10% crustal assimilation.

The Pb isotopic compositions of whole rocks and feldspars from the layered gneiss, Webb Canyon gneiss, and Rendezvous gabbro (Table 6) are typical of isotopic compositions from other regions of the Wyoming Province, and they plot well above the upper crustal model curve of Zartman and Doe (1981) (Fig. 12). We do not have any analyses from the MBG. Even the Pb isotopic composition of the metasediment with the most radiogenic Nd values (sample 98T8) has elevated $^{207}Pb/^{204}Pb$, which we interpret to indicate at least partial derivation of the sediment from Wyoming Province sources.

Discussion

2.67–2.68 Ga event in the Wyoming Province

Events dating from 2.67 to 2.68 Ga are widespread across the western Wyoming Province. The major deformation that occurred in both the Teton and the Wind River ranges is constrained to have occurred after 2679 Ma in the Wind River Range, the youngest possible age of the folded mafic dikes, and before 2671 Ma in the Teton Range, the youngest possible age for the Webb Canyon gneiss. The Bridger batholith (2670 ± 13 Ma) could be coeval with the 2668 ± 10 Ma Rendezvous gabbro but, because of the large uncertainty about the age, its date only poorly constrains deformation in the Wind River Range. The Rendezvous gabbro constrains the timing of calc-alkalic magmatism in the Teton Range, which is similar to the 2670 ± 3 Ma calc-alkalic magmatism in the Madison Range of southwestern Montana (Mueller et al. 1993). Both ages are consistent with the age of the calc-alkalic Bridger batholith in the Wind River Range.

Tectonic boundary in the Teton Range

The relations we have observed in the Teton Range suggest that the contact between the layered gneiss and the MBG is a tectonic boundary. We base this conclusion on several pieces of evidence. The strongest evidence is the distinct difference in metamorphic grade between the MBG and the layered gneiss. Evidence for granulite facies metamorphism is widespread in the MBG but absent elsewhere in the Teton Range. The high pressure of this metamorphism (P > 0.8 GPa) is consistent with continent–continent collision. Because the kyanite in this gneiss lies parallel to the f_2 fold axes, this

Table 3. Analyses of mafic rocks from the Teton Range and Owl Creek Mountains.

	Rendezvous gabbro		Amphibolite from LG	Owl Creek mafic dikes						
Sample:	98T-11	98T-12	99T-2	98OC3	98OC10A	98OC11A	98OC11B	98OC15	98OC23C	98OC25A
SiO_2 (wt.%)	48.00	47.70	50.10	51.70	49.00	49.70	49.10	48.90	48.90	49.60
TiO_2	0.42	0.26	1.30	0.58	1.07	1.10	2.29	0.90	0.89	0.99
Al_2O_3	24.70	26.30	13.80	12.30	15.10	14.30	12.60	15.00	14.90	15.10
Cr_2O_3	0.04	0.03	0.04							
$Fe_2O_3^T$	4.57	4.09	13.30	11.60	11.90	13.40	17.60	12.00	13.20	12.40
MnO	0.07	0.06	0.20	0.19	0.18	0.20	0.22	0.10	0.20	0.19
MgO	3.01	2.80	6.98	9.13	8.11	7.44	3.67	8.16	7.58	7.92
CaO	13.00	13.90	10.20	10.70	11.10	10.70	8.16	11.00	10.80	10.90
Na_2O	2.48	2.46	2.55	1.57	2.08	2.08	2.34	1.88	2.04	1.97
K_2O	1.00	0.32	0.92	0.36	0.30	0.30	0.95	0.10	0.12	0.19
P_2O_5	0.06	0.05	0.15	0.06	0.09	0.10	0.21	0.08	0.07	0.09
LOI	1.15	0.35	0.65	0.01	0.20	0.30	1.70	0.20	0.01	0.01
Total	98.50	98.32	100.187	98.2	99.13	99.62	98.84	98.32	98.71	99.36
Trace elements (ppm)										
Y	10	6		16	14	23	30	22	19	25
Rb	67	33		12	8	10	36	4	2	4
Sr	165	169		77	136	91	161	91	85	96
Ba	86	54		101	113	68	244	33	33	64
Zr	36	37		51	64	67	127	52	49	63
Nb	4	16		8	4	2	9	8	2	3
Th	0.6	0.6						1.1		
U	0.3	0.3								

Note: $Fe_2O_3^T$, total iron content shown as Fe_2O_3; LOI, loss on ignition; LG, layered gneiss.

Table 4. Rare-earth element analyses of rocks from the Teton Range and Owl Creek Mountains.

	Layered gneiss		Augen gneiss		Webb Canyon gneiss	Mount Owen Quartz Monzonite				Rendezvous gabbro		Owl Creek dike
Sample:	98T-6	98T-9	99T-1	99T-6	99-T4	98T-17	98T-1	98T-3	98T-19	99T-5	98T11	98T12	98OC15b
La (ppm)	83.9	61.7	54.5	58.7	35.6	70.2	17	45.8	27.7	65.7	3.8	3.6	3.6
Ce	149	110	100	121	74.7	161	36.5	91.7	64.5	140	8.1	7.9	9.7
Pr	16.1	11.6	10.5	13	8.3	20	4.2	9.2	7.6	16.8	1	1	1.7
Nd	57.9	41.6	34.9	44.9	32.8	90.9	16	36.1	30.3	55.7	4.6	4.8	7.4
Sm	11.6	8.1	7.6	8.9	6.5	24.5	5.1	8.1	9.2	11.5	1.2	1.2	3.1
Eu	1.79	1.85	1.66	1.77	0.96	3.31	0.44	1.51	0.68	1.06	0.51	0.57	1.05
Gd	10.6	8.1	7	7	5.6	28.5	5.3	9.4	8.9	9.7	1.5	1.5	3.3
Tb	1.4	1.1	1	0.9	0.6	4.3	0.8	1.3	1.4	1.2	0.2	0.2	0.06
Dy	7.1	5.4	5.7	3.7	2.9	28.1	5.1	9	8.5	5.5	1.4	1.5	3.9
Ho	1.29	0.94	1.11	0.62	0.46	5.38	0.94	1.77	1.57	1.01	0.29	0.3	0.77
Er	3.2	2.4	3.1	2.2	1.2	16.3	3	5.2	4.5	3	0.9	0.9	2.8
Tm	0.4	0.3	0.5	0.2	0.1	2.1	0.4	0.7	0.6	0.4	0.1	0.1	0.04
Yb	2.8	2.3	2.5	1.5	0.9	14.3	2.5	4.4	3.3	2.3	0.9	0.9	2.6
Lu	0.42	0.32	0.4	0.22	0.12	1.98	0.34	0.61	0.45	0.34	0.12	0.13	0.4

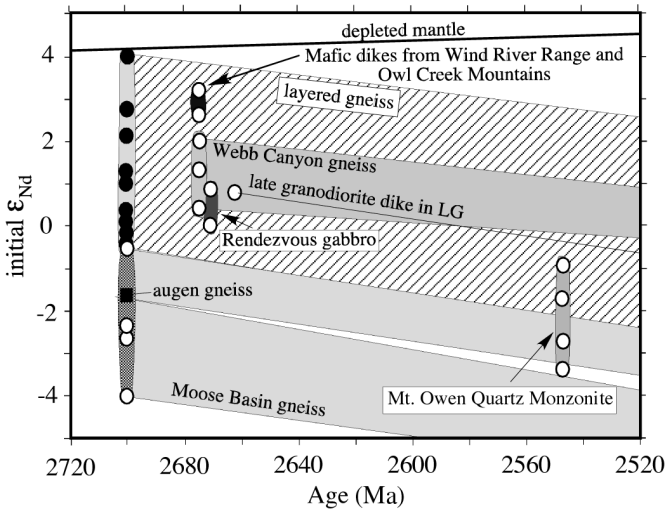

Fig. 11. ε_{Nd} vs. age diagram for rocks from the Teton Range, the Wind River Range, and western Owl Creek Mountains. LG, layered gneiss.

metamorphism clearly occurred at the same time as the emplacement of the magmas forming the Webb Canyon gneiss.

The differences in Nd isotopic signature between the metasedimentary rock in the layered gneiss and MBG (Fig. 11) also support this theory. The pelitic metasediments of the MBG have ε_{Nd} ranging from –0.6 to –4.1, suggesting that they were derived mainly from a continental source. The layered gneiss, in contrast, lacks pelitic units. For the most part, it is not possible to determine if layers in it are orthogneisses or paragneisses. The one Qtz–Bt–Pl schist we are reasonably certain is a paragneiss is chemically immature and has ε_{Nd} of 4.1. This is one of the most radiogenic ε_{Nd} of any metasedimentary rocks from the Wyoming Province. It has elevated $^{207}Pb/^{204}Pb$, typical of the Wyoming Province however, reflecting either partial derivation from a high-μ ($^{238}U/^{204}Pb$) mantle reservoir or contributions of >3.6 Ga detritus (Frost et al. 2006*a*). In light of the radiogenic Nd data, we favor a high-μ, Wyoming Province, mantle source for the Pb and Nd in this rock. The only other metasedimentary rocks from the Wyoming Province that have such positive ε_{Nd} are metagreywackes interpreted to have been accreted to the craton at ca. 2.65 Ga (Frost et al. 2006*b*). The primitive chemical and Nd isotopic compositions of the paragneiss in the layered gneiss suggests that the metasedimentary rocks of the layered gneiss could have formed as an accretionary prism that was partially melted and intruded by arc magmas.

Origin of the Webb Canyon gneiss

The distinctive major element and trace element composition of the Webb Canyon gneiss suggests that it was formed by partial melting of crustal rocks. The Webb Canyon gneiss is silica rich and shows a wide range in MALI, Fe*, and ASI, similar to the peraluminous leucogranites compiled by Frost et al. (2001) that clearly formed as crustal melts. Because the Webb Canyon gneiss is weakly peraluminous to metaluminous, the source rocks for it cannot have been pelitic. The most peraluminous members of the Webb Canyon gneiss have an ASI of 1.1, approximately that of some of the melts

Table 5. Nd and Sr isotopic data for Archean rocks from the Teton Range, western Owl Creek Mountains, and Washakie block of the Wind River Range.

Sample	Rb (ppm)	Sr (ppm)	$\frac{^{87}Rb}{^{86}Sr}$	$\frac{^{87}Sr}{^{86}Sr}$	Initial $\frac{^{87}Sr}{^{86}Sr}$	Sm (ppm)	Nd (ppm)	$\frac{^{147}Sm}{^{144}Nd}$	$\frac{^{143}Nd}{^{144}Nd}$	Initial $\frac{^{143}Nd}{^{144}Nd}$	Initial ε_{Nd}	Nd model age (Ga)
Moose Basin gneiss, Teton Range, initials calculated at 2700 Ma												
T2–31B*	30.65	59.24	1.5058	0.76731	0.71068	1.842	8.939	0.1246	0.511146	0.508927	–4.1	3.4
T2–34A*	9.395	130.3	0.2088	0.71465	0.7068	2.436	10.54	0.1398	0.511499	0.509009	–2.4	3.4
T2–34G*	13.29	99.3	0.3879	0.72230	0.70771	2.725	13.77	0.1196	0.511234	0.509103	–0.6	3.1
T2–34H*	7.016	190.0	0.1069	0.71000	0.70598	1.999	10.54	0.1146	0.511037	0.508995	–2.7	3.2
Layered gneiss, Teton Range, initials calculated at 2700 Ma												
T35E*	43.79	92.42	1.3758	0.74272	0.69098	4.523	24.81	0.1102	0.511063	0.509101	–0.7	3.1
T46A*	51.89	105.8	1.4284	0.77058	0.71686	3.873	22.71	0.1031	0.511074	0.509237	2.0	2.9
T84*	20.5	101.6	0.5901	0.81750	0.79531	10.64	51.91	0.1239	0.511343	0.509136	0.0	3.1
T32A*	53.59	132.9	1.1731	0.76280	0.71868	21.20	85.26	0.1504	0.511802	0.509124	–0.2	3.2
T46B*	57.12	42.73	3.9353	0.88422	0.73621	4.364	12.13	0.2176	0.512988	0.509111	–0.4	
T57*	4.83	207.3	0.0674	0.70450	0.70197	4.040	24.05	0.1015	0.511055	0.509246	2.2	2.8
T77E*	22.47	137.7	0.4729	0.72232	0.70453	2.707	16.98	0.0964	0.510915	0.509197	1.2	3
99T-2	20.5	91.46	0.6498	0.72676	0.70232	3.581	13.45	0.1609	0.511996	0.509129	–0.1	
98T6	48.65	108.2	1.308	0.76436	0.71517	10.89	55.19	0.1192	0.511309	0.509185	1.0	3
98T7	88.57	65.81	3.9788	0.92832	0.77868	26.81	119.2	0.1360	0.511702	0.509279	2.8	2.8
98T8	96.12	119.26	2.3554	0.80890	0.72031	48.12	228.0	0.1276	0.511617	0.509344	4.1	2.7
98T9	69.55	159.55	1.2671	0.75382	0.70616	5.032	25.89	0.1175	0.511287	0.509194	1.2	2.9
Augen gneiss, Teton Range, initials calculated at 2700 Ma												
99T-6	81.39	174.1	1.3606	0.76480	0.71362	6.490	37.40	0.1049	0.510914	0.509045	–1.8	3.1
98T-4	78.61	153.5	1.4920	0.77709	0.72097	7.149	36.24	0.1192	0.511169	0.509044	–1.8	3.2
Webb Canyon gneiss, Teton Range, initials calculated at 2673 Ma												
98T-17	33.71	31.25	3.1653	0.85023	0.73118	27.78	104.5	0.1600	0.512057	0.509233	1.3	
98T-16	34.44	84.62	1.1833	0.75596	0.71146	44.07	166.5	0.1601	0.512013	0.509187	0.4	
4–21B*	76.55	19.65	11.843	1.22288	0.77746	7.807	34.08	0.1385	0.511713	0.509268	2.0	2.9
Rendezvous gabbro, Teton Range, initials calculated at 2668 Ma												
98T-11	54.66	160.3	0.9892	0.73042	0.69322	1.306	4.972	0.1588	0.512014	0.509214	0.9	
98T-12	41.41	173.1	0.6934	0.72461	0.69853	1.157	4.780	0.1464	0.511748	0.509168	0.0	3.2
Granodiorite sill in western layered gneiss, Teton Range, initials calculated at 2663 Ma												
99T1	42.94	186.4	0.6682	0.73012	0.70499	5.612	30.1	0.1127	0.511206	0.509226	0.9	2.9
Mount Owen Quartz Monzonite, Teton Range, initials calculated at 2547 Ma												
98T-1	125.5	33.03	11.528	1.20451	0.77096	5.231	18.33	0.1725	0.512185	0.509287	–0.9	
98T-3	48.18	115.4	1.214	0.76124	0.71558	7.468	34.01	0.1328	0.511476	0.509246	–1.7	3.1
98T-19	165.6	52.49	9.476	1.09526	0.73887	8.372	29.51	0.1715	0.512076	0.509195	–2.7	
99T-5	131.2	92.19	4.195	0.90234	0.74455	9.142	47.00	0.1176	0.511141	0.509166	–3.3	3.2
Mafic dike, western Owl Creek Mountains, initials calculated at 2683 Ma												
98OC15b	1.538	83.28	0.0534	0.70315	0.70108	1.879	6.045	0.1880	0.512643	0.509319	3.1	
Mafic dike, Washakie block, Wind River Range, initials calculated at 2681 Ma												
95BOB20	9.057	95.94	0.2732	0.71052	0.69935	1.949	6.382	0.1847	0.512653	0.509119	–2.9	

Note: *, sample reported in Miller et al. 1986. Analytical details: ~80–100 mg of sample were dissolved in HF–HNO_3. After conversion to chlorides, one-third of the sample was spiked with ^{87}Rb, ^{84}Sr, ^{149}Sm, and ^{146}Nd. Rb, Sr, and rare-earth elements were separated by conventional cation-exchange procedures. Sm and Nd were further separated in di-ethyl-hexyl orthophosphoric acid colums. All isotopic measurements were made on a VG Sector multi-collector mass spectrometer at the University of Wyoming, Laramie. An average $^{87}Sr/^{86}Sr$ isotopic ratio of 0.710251 ± 20 (2σ) was measured for NBS 987 Sr, and an average $^{143}Nd/^{144}Nd$ ratio of 0.511846 ± 11 (2σ) was measured for the LaJolla Nd standard. Uncertainties in Sr isotopic ratio measurements are ±0.00002 and uncertainties in Nd isotopic ratio measurements are ±0.00001 (2σ). Blanks are <50 pg for Rb, Sr, Nd, Sr, and no blank correction was made. Uncertainties in Rb, Sr, Nd, and Sm concentrations are ±2% of the measured value; uncertainties on initial ε_{Nd} = ±0.5 epsilon units. Initial Sr and Nd isotopic ratios and initial ε_{Nd} values are calculated for 170 Ma. Nd model ages are calculated based upon the depleted mantle model of Goldstein et al. 1984 for samples with $^{147}Sm/^{144}Nd < 0.15$.

Table 6. Pb isotopic results of Archean rocks from the Teton Range.

Sample	$\frac{^{206}Pb}{^{204}Pb}$	$\frac{^{207}Pb}{^{204}Pb}$	$\frac{^{208}Pb}{^{204}Pb}$	U (ppm)	Pb (ppm)	$\frac{^{238}U}{^{204}Pb}$	Initial $\frac{^{206}Pb}{^{204}Pb}$	Initial $\frac{^{207}Pb}{^{204}Pb}$
Eastern layered gneiss, Teton Range, initials calculated at 2700 Ma								
T35E wr	20.621	16.254	48.676	0.08	6.2	1.0	20.102	16.158
T46B wr	20.338	16.184	34.759	5.09	43.3	7.3	16.52	15.476
T84 wr	18.475	15.918	43.679	4.4	51.5	5.8	15.437	15.355
T32A wr	50.679	21.248	70.662	8.67	17.5	61.3	18.782	15.341
T46A wr	19.566	16.018	40.414	1.47	16.5	5.9	16.479	15.446
T77E wr	23.953	16.821	47.556	1.94	13.6	11	18.247	15.764
98T6 wr	23.356	16.79	62.595	4.16	31.8	11.74	17.251	15.659
98T7 wr	36.117	19.112	46.584	8.43	42	17.8	26.837	17.393
98T8 wr	26.662	17.396	49.026	5.37	17	25.7	13.289	14.919
Model Wyoming Province mantle at 2.70 Ga						8.5	13.678	14.991
98T9 wr	19.98	16.223	45.937	2.12	20.7	7.4	16.137	15.511
Augen gneiss, Teton Range, initials calculated at 2700 Ma								
99T-6 fld	14.546	15.179	36.437					
98T4 wr	16.024	15.383	43.334	1.25	30.1	2.7	14.613	15.122
Webb Canyon gneiss, Teton Range, initials calculated at 2676 Ma								
98T17 fld	32.192	20.527	51.532					
98T17 wr	85.33	28.18	119.045	5.29	9.9	107.5	30.032	18.086
Rendevous gabbro, Teton Range, initials calculated at 2672 Ma								
98T11 wr	18.305	15.97	31.604	0.47	3	9.3	13.536	15.102
98T12 fld	14.713	15.238	34.04					
98T12 wr	16.881	15.621	35.75	0.27	3.9	4.1	14.765	15.236
Mount Owen Quartz Monzonite, Teton Range, initials calculated at 2547 Ma								
98T1 wr	25.315	17.057	37.987	4.19	37.9	7.8	21.55	16.421
98T3 wr	33.966	18.675	53.852	4.97	22.4	20.6	23.99	16.989
98T19 wr	22.43	16.498	39.226	13.38	81.6	11.2	16.999	15.581

Note: Wyoming Province model mantle reservoir values at 2.70 Ga calculated after Luais and Hawkesworth (2002) using whole-rock Pb isotopic values from sample 98T8 and single-stage growth from Canyon Diablo meteorite values. Sample 98T8 has near mantle ε_{Nd} values at 2.70 Ga. wr, whole rock; fld, feldspar. Analytical details: Pb and U were purified in the feldspar and whole-rock samples using HCl–HBr chemistry, modified from Tilton (1973). Pb and U samples were loaded onto single rhenium filaments with silica gel and graphite, respectively, for isotopic analysis on a VG Sector 54 mass spectrometer. Mass discrimination factors of 0.068% ± 0.08% for Pb and 0% ± 0.06% for U were determined by multiple analyses of NBS SRM 981 and U-500 respectively. PBDAT (Ludwig 1988) was used to reduce raw mass spectrometer data, correct for blanks, and calculate uncertainties, which are 0.16%, 0.24%, and 0.32% on $^{206}Pb/^{204}Pb$, $^{207}Pb/^{204}Pb$, and $^{208}Pb/^{204}Pb$, respectively. $^{208}Pb/^{235}U$ tracer used to measure U and Pb concentrations and $^{238}U/^{204}Pb$ was calibrated against MIT2 gravimetric standard and yielded a $^{206}Pb/^{238}U$ date of 419.26 ± 0.47 Ma for zircon standard R33 in good agreement with ROM date (Black et al. 2004).

produced from model greywackes by Patino Douce and Beard (1996). The melting of small amounts of amphibole may have produced the metaluminous melts. This is suggested by the fact that the ASI of the Webb Canyon gneiss is inversely correlated with Na_2O content. The most metaluminous rocks are true tonalites with >5.0 wt.% Na_2O, igneous rocks that are commonly ascribed to melting of hornblende-bearing sources (Martin et al. 2005).

The high REE and Zr contents of the Webb Canyon gneiss also suggest derivation via high temperature, partial melting of a zircon-bearing sediment. The high Zr content of the Webb Canyon gneiss suggests two things. First, it indicates that the protolith to the gneiss was emplaced at high temperatures. Zircon-saturation temperatures for Webb Canyon gneiss are >900 °C, but those temperatures are clearly an overestimate because, as noted in the geochronology section, the zircon population from the Webb Canyon gneiss contains a considerable component of inheritance (Fig. 6A). However, even if 25% of the Zr is from cumulate or inherited zircons, the magmatic temperatures for these rocks will still be 900 °C or greater. Second, it implies that the silica-rich composition of the Webb Canyon gneiss is not a result of differentiation; if it were, the fractionation of zircon would have depleted Zr from the rock.

If the Webb Canyon gneiss is a product of crustal melting, it was not produced by melting of pelitic horizons of the MBG. Not only would melting of pelitic rock produce a strongly peraluminous granite, but it would also have produced a rock with a substantially lower initial ε_{Nd} (Fig. 11). However, the layered gneiss, which contains a wide range of rock types, including amphibolites, has an isotopic composition consistent for a source for the Webb Canyon gneiss.

Fig. 12. Pb isotopic compositions of whole-rock samples and step-dissolved feldspars from Archean rocks of the Teton Range. The model upper crust and mantle curves of Zartman and Doe (1981) are plotted for reference. The Pb isotopic compositions of feldspars from the western Owl Creek Mountains (OC) (Frost et al. 2006*a*) plot in the field labeled "O", eastern Beartooth Mountains (EBT) (Wooden and Mueller 1988) in "E", and the Wind River Range (WR) (Frost et al. 1998) in "W". Calculated Pb isotopic initial compositions of whole-rock samples from the Beartooth–Bighorn Magmatic Zone (BBMZ) plot within the dark shaded field (Frost et al. 2006*a*). High-μ ($^{238}U/^{204}Pb$) model mantle reservoir for the Wyoming Province is plotted after Luais and Hawkesworth (2002) and Frost et al. (2006*a*). A model mantle Pb value for the Teton Range is calculated from the Pb isotopic composition of 98T8, the layered gneiss sample with depleted mantle Nd values, following the method of Luais and Hawkesworth (2002). Pb isotopic data from whole rocks plot in a broad swath that projects back to the measured feldspar values from the Teton Range and the fields defined by other regions of the Wyoming Province (WY), consistent with derivation from similar sources. There are no data from the Moose Basin gneiss however. Many of the whole-rock measurements are extremely radiogenic and plot off the scale of the figure, but they still fall within the extension of the swath shown.

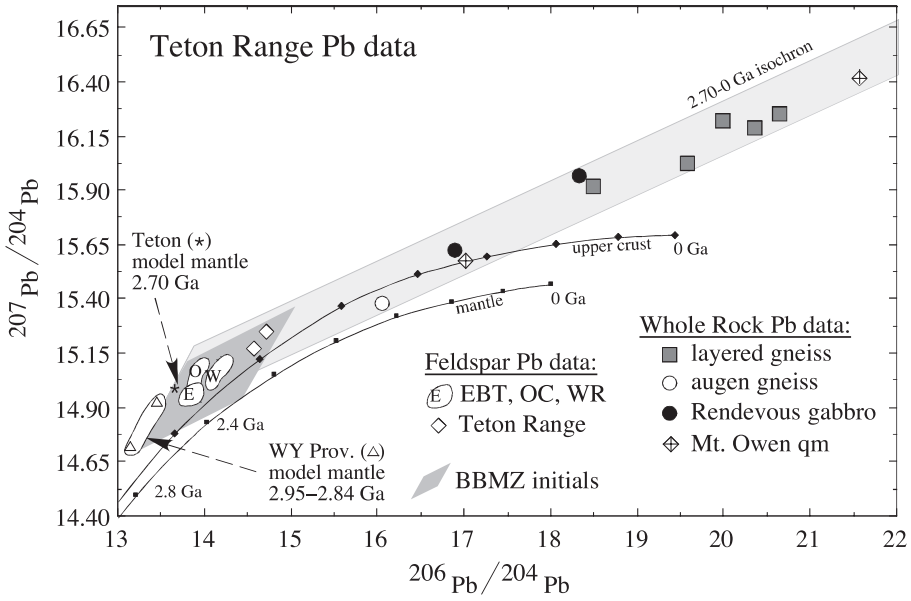

Origin of the Bridger batholith and the Rendezvous gabbro

Unlike the Webb Canyon gneiss, which is likely to be a crustal melt, the Bridger batholith and the Rendezvous gabbro appear to have formed in magmatic arc settings. The calc-alkalic trend of the Bridger batholith is typical of a Cordilleran batholith (Frost et al. 2001). More importantly, the Bridger batholith has a range of Nd isotopes indicating that it is composed of both crustal and juvenile components (Frost et al. 1998). The calc-alkalic composition of the Rendezvous gabbro suggests that it too formed in a magmatic arc. The Nd isotopic composition of the Rendezvous gabbro is not as radiogenic as melts that are solely mantle derived because this intrusion has low REE abundances. Addition of small amounts of crustal contamination would significantly affect its Nd isotopic composition. Crustal assimilation is also indicated in the U–Pb zircon data, which we interpret to indicate inheritance of grains that are at least 20 Ma older than the gabbro.

Origin of the 2.55 Ga Mount Owen Quartz Monzonite

The tectonic environment of the 2.55 Ga Mount Owen Quartz Monzonite, which represents the last Archean plutonic event in the Teton Range, is unknown. Its hydrous, peraluminous composition suggests that it formed from crustal melting of pelitic or psammitic metasedimentary rocks, but there is no evidence of penetrative deformation in the Teton Range at this time. Similar 2.55 Ga peraluminous granites are widespread but minor components in the Wyoming Province. They are found in the Teton Range, at South Pass in the Wind River Range (Frost et al. 2006*b*), in the Granite Mountains (Wall 2004), the Laramie Mountains (Wall 2004), and in the Black Hills (McCombs et al. 2004). The Mount Owen Quartz Monzonite was emplaced at the time when the MMP was thrust onto the Beartooth Bighorn domain (Mogk et al. 1988), but it is unclear how this thrusting event could be related to crustal melting that occurred across the Wyoming Province.

Conclusion

Tectonic model for the Wyoming Province at 2.68–2.67 Ga

The available geochronology indicates that the major penetrative deformation in the Wind River and Teton ranges were roughly coeval at around 2670–2680 Ma. Based upon the structural relations, the metamorphic conditions, and the whole-rock and isotopic geochemistry of the rocks in the two ranges, we conclude that active-margin tectonics dominated the western edge of the Wyoming Province at this time (Fig. 13). The cross-section in Fig. 13 is drawn approximately along line A–A′ in Fig. 1. The distance across this section is ~150–200 km. The true distance in the Archean is not known because we do not know if rocks similar to those in the Teton Range lie buried to the southwest of the Wind

Fig. 13. Proposed tectonic environment of the western Wyoming Province between 2680 and 2670 Ga. constructed along the line A–A′ in Fig. 1.

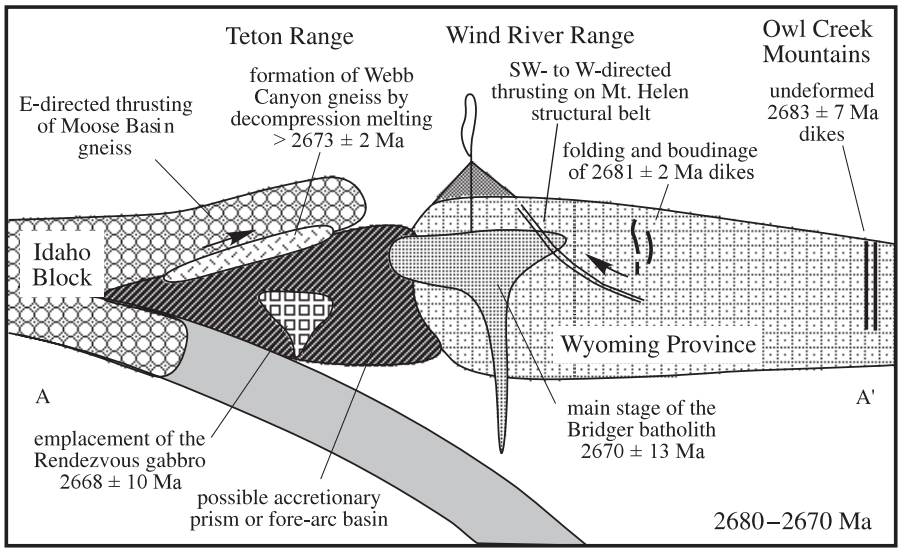

River Range, nor do we know the extent to which the geologic features in the two ranges have been displaced by Laramie deformation.

We contend that the 2670–2680 Ma deformation event was the product of east- or northeast-directed subduction beneath the western margin of the Wyoming Province. This is indicated by the calc-alkalic compositions and juvenile isotopic signatures of the Rendezvous gabbro and Bridger batholith. In such a model, the dike swarm in the Owl Creek Mountains and the eastern Wind River Range formed in a back-arc environment. The relatively primitive rocks of the layered gneiss in the Teton Range could represent either an accretionary wedge or a fore-arc basin constructed on the western margin of the Wyoming Province, into which a substantial proportion of immature primitive sediments accumulated. These rocks were then metamorphosed, partially melted, and intruded by arc-related magmas. A possible example of one of these magmas would be the augen gneiss.

The climax of this orogenic cycle occurred during the collision of a continental block from the west or southwest with the main Wyoming Province. We call this cryptic continental block the Idaho block and infer its presence for two reasons. First the MBG has been subjected to high-pressure metamorphism and the most likely environment for producing such high-pressure metamorphism is during continental collisions (Thompson and England 1984). Second, the MBG has Nd model ages around 3.3 Ga, which are similar to the Archean xenoliths from the Snake River Plain, which also have 3.5 Ga model ages (Leeman et al. 1985; Wolf et al. 2005).

We propose that the Webb Canyon gneiss was produced by decompression melting and intruded along this proposed thrust late during deformation. It is evident that the Webb Canyon gneiss was emplaced during deformation because its foliations and lineations are parallel to the limbs and axes of the f_2 folds. If the Webb Canyon gneiss was formed by this process, it must have been derived from the footwall because it is isotopically distinct from the more evolved rocks of the MBG.

In the Wind River Range, the orogenic climax produced southwest thrusting along the MHSB, which boudinaged and metamorphosed the 2680 Ma mafic dikes in the hanging wall. The MHSB, itself, was truncated by the Bridger batholith, which carries the northwest-trending foliation of the MHSB. Because portions of the Bridger batholith are isotopically primitive, some of the sources for the batholith must have been derived from the mantle or from a young subducted plate. The metamorphic conditions (675–700 °C, 4.5–4 kbar (1 kbar = 100 MPa)) (Frost et al. 2000*a*; Donohue and Essene 2005) associated with the MHSB are also consistent with metamorphism that is driven by magmatic heating and that is distinctly different from the metamorphic conditions in the MBG of the Teton Range.

The final intrusive event in the 2.68–2.67 Ga orogeny was the emplacement of the Rendezvous gabbro at 2668 Ma. By this timem, penetrative deformation had ceased in the orogeny. Because the Rendezvous metagabbro has a calc-alkalic affinity and a relatively radiogenic initial Nd isotopic signature, it was probably formed in a subduction environment and we interpret it as an arc pluton. Thus, we conclude that most of the Idaho block was obducted during this orogeny, rather than subducted.

The orogenic events along the western and southwestern margin of the Wyoming Province appear to be distinct in time from similar orogenic events in the eastern Sweetwater subprovince. Lateral accretion, deformation, and magmatic modification in the southern Wind River Range and Granite Mountains have been documented from 2.65 to 2.63 Ga (Frost et al. 1998; Chamberlain et al. 2003; Grace et al. 2006; Frost et al. 2006*b*). Combined with the evidence in this study, these events clearly establish operation of plate-tectonic style processes in western and southern Wyoming Province in the late Archean.

Relation to other Archean provinces

Perhaps the best example of Archean high-pressure metamorphism that is similar to that found in the Teton Range is in the Kaapvaal craton of South Africa. The Kaapvaal craton was assembled between 3.6 and 3.2 Ga. Between 3.1 and

3.0 Ga, Cordilleran-type plutons were emplaced in an arc that extends across the northern and western margins of the craton. Poujol et al. (2003) ascribe these plutons to a magmatic arc that was built upon the older craton. Additional Cordilleran-type plutons were emplaced between 3.0 and 2.7 Ga during arc–continent collisions. At 2.7 Ga, the Limpopo belt was formed during the collision between the Kaapvaal and the Zimbabwe cratons (van Reenen et al. 1987).

The Limpopo belt is a complex tectonic zone consisting of three zones: the Northern Marginal Zone (NMZ), the Central Zone (CZ), and Southern Marginal Zone (SMZ). The Archean history is best recorded in the NMZ and SMZ because structures and mineral assemblages in the CZ were modified by Proterozoic transpressive deformation that produced granulite metamorphism up to 12 kbar (Holzer et al. 1998). U–Pb monazite dating from the SMZ indicates that an earlier phase of granulite metamorphism (~850 °C, ~8 kbar) occurred at 2691 ± 7 Ma and that this metamorphism is coeval with southward thrusting of the Limpopo belt over the Kaapvaal craton (Kressig et al. 2001). This deformation was either prolonged or episodic and continued at least until 2643 ± 1 Ma, which is the age of a leucosome from the SMZ (Kressig et al. 2001).

The geologic relations in the Wyoming Province and in South Africa indicate that modern-day plate tectonic process—construction of magmatic arcs on preexisting continental crust, back-arc rifting, and continent–continent collisions producing contractional fabrics and high-pressure metamorphism—were operating by 2.7 Ga. This calls into question the plume-related global "crisis" postulated by Rey et al. (2003) to account for the voluminous late Archean (2.75–2.65 Ga) plutonism. If such a plume-driven process was operating, it surely missed the Wyoming Province, where all plutons in this time range have a restricted distribution and are clearly related to contractional fabrics.

Structures in middle Archean terranes can be convincingly ascribed to vertical tectonics (as in the Pilbara, Van Kranendonk et al. 2004), and may have operated in the Neoarchean (Bédard et al. 2003); we have noted that horizontal tectonics were operating in the Limpopo belt and in the Wyoming Province by 2.68 Ga. However, we hesitate to say that horizontal tectonics constituted the dominant tectonic process in the late Archean. In some cratons, late Archean calc-alkalic plutons are not arranged in linear belts. For example, in the Slave Province, Davis and Bleeker (1999) recognize five pulses of plutonism between 2.63 and 2.58 Ga. Plutons from each pulse are distributed across the whole Slave Province, and there is no compelling reason to attribute any of these plutons to subduction-related tectonics.

Much of the central Wyoming Province is composed of 3.0 to 2.84 Ga tonalite, granodiorite, and granite that does not appear to have been formed in an environment similar to modern-day plate tectonics (Frost et al. 2006). However, as noted in Fig. 13, the 2.68–2.67 Ga plutonic and tectonic events on the western margin of the province can be reasonably modeled by modern plate tectonics. This implies that the transition from vertical tectonics, which appears to have been prevalent early in the Earth's history (Hamilton 1998), to modern-day horizontal plate tectonics may have lasted for hundreds of millions of years and may have taken place at different times in different cratons.

Acknowledgements

Research was funded by National Science Foundation grant EAR 9909260 to C.D. Frost, K.R. Chamberlain, and B.R. Frost, and National Park Service – University of Wyoming research grants to K.R. Chamberlain, C.D. Frost, and B.R. Frost. Jessica Scott Anderson and Peter Valley provided technical assistance with some of the U–Pb geochronologic analyses. We also wish to thank Marc LaFlèche, Paul Mueller, and Michael Palin for helpful reviews of a previous version of this text.

References

Aleinikoff, J.N., Williams, I.S., Compston, W., Stuckless, J.S., and Worl, R.G. 1989. Evidence for an early Archean component in the Middle to Late Archean gneisses of the Wind River Range, west-central Wyoming: conventional and ion microprobe U–Pb data. Contributions to Mineralogy and Petrology. **101**: 198–206.

Barker, F. Millard, H.T., and Lipman, P.W. 1979. Four low-K siliceous rocks of the western USA. *In* Trondhjemites, dacites, and related rocks, *Edited by* F. Barker. Elsevier, New York, N.Y., pp. 415–434.

Barton, J.M., Doig, R., Smith, C.B., Bohlender, F., and van Reenen, D.D. 1992. Isotopic and REE characteristics of the intrusive charnoenderbite and enderbite geographically associated with the Matok pluton, Limpopo belt, southern Africa. Precambrian Research, **55**: 451–467.

Bédard, J.H., Brouillette, P., Madore, L., and Berclaz, A. 2003. Archaean cratonization and deformation in the northern Superior Province, Canada: an evaluation of plate tectonic versus vertical tectonic models. Precambrian Research, **127**: 61–87.

Black, L.P., Kamo, S.L., Allen, C.M., Davis, D.W., Aleinikoff, J.N., Valley, J.W., et al. 2004. Improved $^{206}Pb/^{238}U$ microprobe geochronology by the monitoring of a trace-element-related matrix effect; SHRIMP, ID–IMS, ELA–IP–S and oxygen isotope documentation for a series of zircon standards. Chemical Geology, **205**: 115–140.

Card, K.D. 1990. A review of the Superior province of the Canadian Shield, a product of Archean accretion. Precambrian Research, **48**: 99–156.

Chamberlain, K.R. Frost, C.D., and Frost, B.R. 2003. Early Archean to Mesoproterozoic evolution of the Wyoming Province: Archean origins to modern lithospheric architecture. Canadian Journal of Earth Sciences, **40**: 1357–1374.

Cornia, M.E. 2003. The Archean history of the Teton Range and surrounding areas, Wyoming and Idaho. Unpublished M..Sc. thesis, University of Wyoming, Laramie, Wyo.

Davis, W.J., and Bleeker, W. 1999. Timing of plutonism, deformation, and metamorphism in the Yellowknife domain, Slave Province, Canada. Canadian Journal of Earth Sciences, **36**: 1169–1187.

Donohue, C.L., and Essene, E.J. 2005. Granulite facies conditions preserved in vanadium- and chromium-rich metapelites from the Paradise Basin, Wind River Range, Wyoming, USA. Canadian Mineralogist, **43**: 495–511.

Ellis, D.J. 1992. Precambrian tectonics and the physiochemical evolution of the continental crust. II. Lithosphere delamination and ensialic orogeny. Precambrian Research, **55**: 507–524.

Frost, B.R., Chamberlain, K.R., Swapp, S., Frost, C.D., and Hulsebosch, T.P. 2000*a*. Late Archean structural and metamorphic history of the Wind River Range: Evidence for a long-lived active margin on the Archean Wyoming craton. Geological Society of America Bulletin, **112**: 564–578.

Frost, B.R., Frost, C.D., Hulsebosch, T.P., and Swapp, S.M. 2000*b*.

Origin of the Louis Lake batholith, Wind River Range, Wyoming. Journal of Petrology, **41**: 1759–1776.

Frost, B.R., Arculus, R.J., Barnes, C.G., Collins, W.J., Ellis, D.J., and Frost, C.D. 2001. A geochemical classification of granitic rocks. Journal of Petrology, **42**: 2033–2048.

Frost, C.D., Frost, B.R., Chamberlain, K.R., and Hulsebosch, T.P. 1998. The Late Archean history of the Wyoming Province as recorded by granitic magmatism in the Wind River Range, Wyoming. Precambrian Research, **89**: 145–173.

Frost, C.D., Frost, B.R., Kirkwood, R., and Chamberlain, K.R. 2006*a*. The tonalite–trondjhemite–granodiorite (TTG) to granodiorite–granite (GG) transition in the late Archean plutonic rocks of the central Wyoming Province. Canadian Journal of Earth Sciences, **43**: this issue.

Frost, C.D., Fruchey, B.J., Chamberlain, K.R., and Frost, B.R. 2006*b*. Archean crustal growth by lateral accretion of juvenile supracrustal belts in the south-central Wyoming Province. Canadian Journal of Earth Sciences, **43**: this issue.

Grace, R.L.B., Chamberlain, K.R., Frost, B.R., and Frost, C.D. 2006. Tectonic histories of the Paleo- to Mesoarchean Sacawee block and Neoarchean Oregon Trail structural belt of south-central Wyoming Province. Canadian Journal of Earth Sciences, **43**: this issue.

Hamilton, W.B. 1998. Archean magmatism and deformation were not products of plate tectonics. Precambrian Research, **91**: 143–179.

Harlan, S.S., Geissman, J.W., and Snee, L.W. 1997. Paleomagnetic and $^{40}Ar/^{39}Ar$ geochronologic data from late Proterozoic mafic dikes and sills, Montana and Wyoming. United States Geological Survey Professional Paper 1580.

Hausel, W.D., Graff, P.J., and Albert, K.G. 1985. Economic geology of the Copper Mountain supracrustal belt, Owl Creek Mountains, Fremont, County, Wyoming. Geologic Survey of Wyoming, Report of Investigations 28.

Hedge, C.E., Simmons, K.R., and Stuckless, J.S. 1986. Geochronology of an Archean granite, Owl Creek Mountains, Wyoming. United States Geological Survey, Professonal Paper 1388 B.

Heaman, L.N., and LeCheminant, A.N. 1993. Paragenesis and U–Pb systematics of baddeleyite (ZrO_2). Chemical Geology, **110**: 95–126.

Hildebrandt, P.K. 1989. Petrology, thermobarometry and geochemistry of the Archean layered gneiss, Teton Range, Wyoming. Unpublished M.Sc. thesis, Colorado State University, Fort Collins, Colo.

Holzer, L., Frei, R., Barton, J.M., Jr., and Kramers, J.D. 1998. Unraveling the record of successive high grade events in the Central Zone of the Limpopo belt using Pb single phase dating of metamorphic minerals. Precambrian Research, **87**: 87–115.

Koesterer, M.E., Frost, C.D., Frost, B.R., Hulsebosch, T.P., Bridgwater, D., and Worl, R.G. 1987. Development of the Archean crust in the Medina Mountain area, Wind River Mountains, Wyoming (USA). Precambrian Research, **37**: 287–304.

Kirkwood, R. 2000. Geology, geochronology and economic potential of the Archean rocks in the Western Owl Creek Mountains, Wyoming. Unpublished M.Sc. thesis, University of Wyoming, Laramie, Wyo.

Kressig, K., Holzer, L., Frei, R., Villa, I.M., Kravers, J.D., Kröner, A. et al. 2001. Geochronology of the Hour River shear zone and the metamorphism in the southern marginal zone of the Limpopo belt, Southern Africa. Precambrian Research, **109**: 145.173.

Kretz, R. 1983. Symbols for rock-forming minerals. American Mineralogist, **68**: 27–279.

Krogh, T.E. 1973. A low contamination method for hydrothermal decomposition of zircon and extraction of U and Pb for isotopic age determination. Geochimica et Cosmochimica Acta, **37**: 488–494.

Leeman, W.P., Menzies, M.A., Matty, D.J., and Embree, G.F. 1985. Strontium, neodymiun and lead isotopic compositions of deep crustal xenoliths from the Snake River Plain: evidence for Archean basement. Earth and Planetary Science Letters, **75**: 354–368.

Luais, B., and Hawkesworth, C.J. 2002. Pb isotope variations in Archaean time and possible links to the sources of certain Mesozoic–Recent basalts. *In* The early Earth: physical, chemical and biological development. *Edited by* C.M.R. Fowler, C.J. Ebinger, and C.J. Hawkesworth. Geological Society (of London), Special Publication 199, pp. 105–124.

Ludwig, K.R. l988. PBDAT for MS-DOS, a computer program for IBM–PC compatibles for processing raw Pb–U–Th isotope data, version 1.24. United States Geological Survey, Open-File Report 88-552.

Ludwig, K.R. l991. ISOPLOT for MS-DOS, a plotting and regression program for radiogenic–isotope data, for IBM–PC compatible computers, version 2.75. United States Geological Survey, Open-File Report 91-445.

Martin, H., Smithies, R.H., Rapp, R., Mouen, J.-F., and Champion, D. 2005. An overview of adakite, tonalite–trondjhemite–granodiorite (TTG) and sanukitoid: relationships and some implications for crustal evolution. Lithos, **79**: 1–24.

McCombs, J.A., Dahl, P.S., and Hamilton, M.A. 2004. U–Pb ages of neoaarchean granitoids from the Black Hills, South Dakota, USA: implications for crustal evolution in the Archean Wyoming Province. Precambrian Research, **130**: 161–184.

Miller, S.H., Hildebrandt, P.K., Erlsev, E.A., and Reed, J.C., Jr. 1986. Metamorphic and deformation history of the gneiss complex in the northern Teton Range, Wyoming. *In* Geology of the Beartooth Uplift and Adjacent Ranges, Montana Geologic Society and Yellowstone–Beartooth Research Association Joint Field Conference and Symposium, Red Lodge, Mont., 31 August – 1 September 1986, pp. 91–110.

Mogk, D.W, Mueller, P.A., and Wooden, J.L. 1988. Archean tectonics of the North Snowy Block, Beartooth Mountains, Montana. Journal of Geology, **96**: 125–141.

Mogk, D.W., Mueller, P.A., and Wooden, J.L. 1992. The nature of Archean terrane boundaries: an example from the northern Wyoming province. Precambrian Research, **55**: 155–168.

Mueller, P.A., Peterman, Z.E., and Granath, J.W. 1985. A bimodal Archean volcanic series, Owl Creek Mountains. Journal of Geology, **93**: 701–712.

Mueller, P.A., Shuster, R.D., Wooden, J.L., Erslev, E.A., and Bowes, D.R. 1993. Age and composition of Archean crystalline rocks from the southern Madison Range, Montana: implications for crustal evolution of the Wyoming Craton. Geological Society of America Bulletin, **105**: 437–446.

Parrish, R.R., Roddick, J.C., Loveridge, W.D., and Sullivan, R.D. l987. Uranium–lead analytical techniques at the geochronology laboratory, Geological Survey of Canada. *In* Radiogenic age and isotopic studies, Report 1. Geological Survey of Canada, Paper 87-2, pp. 3–7.

Patino Douce, A., and Beard, J.S. 1996. Effect of P, $f(O_2)$ and Mg/Fe ratio on dehydration melting of model metagreywackes. Journal of Petrology, **37**: 999–1024.

Percival, J.A., and Skulski, T. 2000. Tectonothermal evolution of the northern Minto block, Superior Province, Quebec, Canada. Canadian Mineralogist, **38**: 345–378.

Poujol, M., Robb, L.J., Anhaeusser, C.R., and Gerick, B. 2003. A review of the geochronological constraints on the evolution of the Kaapvaal Craton, South Africa. Precambrian Research, **127**: 181–213.

Reed, J.C., Jr. 1963. Structure of Precambrian crystalline rocks in the northern parat of Grand Teton National Park, Wyoming. *In* Short papers in geology and hydrology. United States Geological Survey, Professional Paper 475-C, pp. C1–C6.

Reed, J.C., Jr. 1973. Geologic map of the Teton Range, Wyoming. United States Geological Survey, Open-File Map 73-230, scale 1 : 62 600.

Reed, J.C., Jr., and Huston, R.S. 1993. Teton and Gros Ventre Ranges. *In* Precambrian: conterminous U.S. *Edited by* J.C. Reed, Jr., M.E. Bickford, R.S. Houston, P.K. Link, D.W. Rankin, P.K. Sims, and W.R. Van Schmus. Geological Society of America, Boulder, Colo., The Geology of North America, Vol. C-2, pp. 133–136.

Rey, P.F., Philippot, P., and Thebaud, N. 2003. Contribution of mantle plumes, crustal thickening and greesntone blanketing to the 2.74–2.65 Ga global crisis. Precambrian Research, **127**: 43–60.

Stacey, J.S., and Kramers, J.D. 1975. Approximation of terrestrial lead isotope evolution by a two-stage model. Earth and Planetary Science Letters, **26**: 207–221.

Steiger, R.H., and Jäger, E. 1977. Subcommission on geochronology: convention on the use of decay constants in geo- and cosmochronology. Earth and Planetary Science Letters, **36**: 359–362.

Stuckless, J.S. Nkomo, R.A., and Ikramuddin, M. 1976. Uranium–thorium–lead systematics of an Archean granite from the Owl Creek Mountains, Wyoming. *In* United States Geological Survey, Professional Paper 1388-C, pp. 39–48.

Stuckless, J.S., Hedge, C.E., Simmons, K.R., Nkomo, I.T., and Wenner, D.B. 1985. Isotope studies of the late Archean plutonic rocks of the Wind River Range, Wyoming. Geological Society of America Bulletin, **96**: 850–860.

Thompson, A.B., and England, P.C. 1984. Pressure–temperature–time paths of regional metamorphism II. Their inference and interpretation using mineral assemblages in metamorphic rocks. Journal of Petrology, **25**: 929–955.

Tilton, G.R. 1973. Isotopic lead ages of chondritic meteorites. Earth and Planetary Science Letters, **19**: 321–329.

Van Kranendonk, M.J., Collins, W.J., Hickman, A., and Pawley, M.J. 2004. Critical tests of vertical vs. horizontal tectonic models for the Archaean east Pilbara granite-greenstone terrane, Pilbara craton, Western Australia. Precambrian Research, **131**: 173–211.

van Reenen, D.D., Barton, J.M. Jr., Roering, C., Smith, C.A., and Van Schalkwyk, J.F. 1987. Deep crustal response to continental collision: the Limpopo belt of southern Africa. Geology, **15**: 11–14.

Wakita, H., Rey, P., and Schmitt, R.A. 1971. Abundances of the 14 rare-earth elements and 12 other trace elements in Apollo 12 samples: five igneous and one breccia rocks and four soils. *In* Proceedings of the 2nd Lunar Science Conference, Vol. 2, pp. 1319–1329.

Wall, E.N. 2004. Petrologic, geochemical and isotopic constraints on the origin of 2.6 Ga post-tectonic granitoids of the central Wyoming Province. Unpublished M.Sc. thesis, University of Wyoming, Laramie, Wyo.

Watson, E.M., and Harrison, T.M. 1983. Zircon saturation revisited: temperature and compositional effects in a variety of crustal magma types. Earth and Planetary Science Letters, **64**: 295–304.

Windley, B.F. 1993. Uniformitarianism today: plate tectonics is the key to the past. Journal of the Geological Society (of London), **150**: 7–19.

Wolf, D.E., Leeman, W.P., and Vervoort, J.D. 2005. U–Pb zircon geochronology of crustal xenolith confirms presence of Archean basement beneath the central and eastern Snake River Plain. Geological Society of America Abstracts with Programs, **37**: 60.

Wooden, J.L., and Mueller, P.A. 1988. Pb, Sr, and Nd isotopic compositions of a suite of Late Archean, igneous rocks, eastern Beartooth Mountains: implications for crust–mantle evolution. Earth and Planetary Science Letters, **87**: 59–72.

Zartman, R.E., and Doe, B.R. 1981. Plumobtectonics—the model. Tectonophysics, **75**: 135–162.

Zartman, R.E., and Reed, J.C. 1998. Zircon geochronology of the Webb Canyon Gneiss and the Mount Owen Quartz Monzonite, Teton Range Wyoming: significance to dating late Archean metamorphism in the Wyoming craton. The Mountain Geologist, **35**: 71–77.